Jinst

PUBLISHED BY INSTITUTE OF PHYSICS PUBLISHING AND SISSA

RECEIVED: *December 21, 2007*
REVISED: *February 1, 2008*
ACCEPTED: *February 5, 2008*
PUBLISHED: *February 29, 2008*

The ATLAS TRT Barrel Detector

The ATLAS TRT collaboration

E. Abat,[a†] T.N. Addy,[j] T.P.A. Åkesson,[m] J. Alison,[u] F. Anghinolfi,[c] E. Arik,[a†] M. Arik,[a] G. Atoian,[z] B. Auerbach,[z] O.K. Baker,[z] E. Banas,[f] S. Baron,[c] C. Bault,[c] N. Becerici,[a] A. Beddall,[a1] A.J. Beddall,[a1] J. Bendotti,[c] D.P. Benjamin,[g] H. Bertelsen,[d] A. Bingul,[a1] H. Blampey,[c] A. Bocci,[g] M. Bochenek,[e] V.G. Bondarenko,[p] V. Bychkov,[l] J. Callahan,[k] M. Capeáns Garrido,[c] L. Cardiel Sas,[c] A. Catinaccio,[c] S.A. Cetin,[a2] T. Chandler,[z] R. Chritin,[h] P. Cwetanski,[k] M. Dam,[d] H. Danielsson,[c] E. Danilevich,[v] E. David,[c] J. Degenhardt,[u] B. Di Girolamo ,[c] F. Dittus,[c] N. Dixon,[c] O.B. Dogan,[a†] B.A. Dolgoshein,[p] N. Dressnandt,[u] C. Driouchi,[d] W.L. Ebenstein,[g] P. Eerola,[m] U. Egede,[m] K. Egorov,[k] H. Evans,[k] P. Farthouat,[c] O.L. Fedin,[v] A.J. Fowler,[g] S. Fratina,[u] D. Froidevaux,[c] A. Fry,[j] P. Gagnon,[k] I.L. Gavrilenko,[o] C. Gay,[y] N. Ghodbane,[r] J. Godlewski,[c] M. Goulette,[c] I. Gousakov,[l] N. Grigalashvili,[l] Y. Grishkevich,[q] J. Grognuz,[c] Z. Hajduk,[f] M. Hance,[u] F. Hansen,[d] J.B. Hansen,[d] P.H. Hansen,[d] G. Hanson,[k3] G.A. Hare,[u] A. Harvey Jr.,[j] C. Hauviller,[c] A. High,[u] W. Hulsbergen,[c] W. Huta,[c] V. Issakov,[z] S. Istin,[a] V. Jain,[k] G. Jarlskog,[m] L. Jeanty,[y] V.A. Kantserov,[p] B. Kaplan,[z] A.S. Kapliy,[u] S. Katounine,[v] F. Kayumov,[o] P.T. Keener,[u] G.D. Kekelidze,[l] E. Khabarova,[l] A. Khristachev,[v] B. Kisielewski,[f] T.H. Kittelmann,[w] C. Kline,[k] E.B. Klinkby,[d] N.V. Klopov,[v] B.R. Ko,[g] T. Koffas,[c] N.V. Kondratieva,[p] S.P. Konovalov,[o] S. Koperny,[e] H. Korsmo,[m] S. Kovalenko,[v] T.Z. Kowalski,[e] K. Krüger,[v] V. Kramarenko,[q] L.G. Kudin,[v] A-C. Le Bihan,[v] B.C. LeGeyt,[u] K. Levterov,[l] P. Lichard,[c] A. Lindahl,[d] V. Lisan,[l] S. Lobastov,[l] A. Loginov,[z] C.W. Loh,[y] S. Lokwitz,[z] M.C. Long,[j] S. Lucas,[c] A. Lucotte,[i] F. Luehring,[k] B. Lundberg,[m] R. Mackeprang,[d] V.P. Maleev,[v] A. Manara,[k] M. Mandl,[c] A.J. Martin,[z] F.F. Martin,[u] R. Mashinistov,[p] G.M. Mayers,[u] K.W. McFarlane,[j] V. Mialkovski,[l] B.M. Mills,[y] B. Mindur,[e] V.A. Mitsou,[x] J.U. Mjörnmark,[m] S.V. Morozov,[p] E. Morris,[k] S.V. Mouraviev,[o] A.M. Muir,[y] A. Munar,[u] A.V. Nadtochi,[v] S.Y. Nesterov,[v] F.M. Newcomer,[u] N. Nikitin,[q] O. Novgorodova,[o] E.G. Novodvorski,[v] H. Ogren,[k*] S.H. Oh,[g] S.B. Oleshko,[v] D. Olivito,[u] J. Olszowska,[f] W. Ostrowicz,[f] M.S. Passmore,[c] S. Patrichev,[v] J. Penwell,[k] F. Perez-Gomez,[c] V.D. Peshekhonov,[l] T.C. Petersen,[c] R. Petti,[b] A. Placci,[c] A. Poblaguev,[z] X. Pons,[c] M.J. Price,[c] O. Røhne,[t] R.D. Reece,[u] M.B. Reilly,[u] C. Rembser,[c] A. Romaniouk,[p] D. Rousseau,[s] D. Rust,[k] Y.F. Ryabov,[v] V. Ryjov,[c] M. Söderberg,[m] A. Savenkov,[l]

2008 JINST 3 P02014

J. Saxon,[u] M. Scandurra,[k] V.A. Schegelsky,[v] M.I. Scherzer,[u] M.P. Schmidt,[z†] C. Schmitt,[c] E. Sedykh,[v] D.M. Seliverstov,[v] T. Shin,[j] A. Shmeleva,[o] S. Sivoklokov,[q] S.Yu. Smirnov,[p] L. Smirnova,[q] O. Smirnova,[m] P. Smith,[k] V.V. Sosnovtsev,[p] G. Sprachmann,[c] S. Subramania,[k] S.I. Suchkov,[p] V.V. Sulin,[o] R.R. Szczygiel,[f] G. Tartarelli,[n] E. Thomson,[u] V.O. Tikhomirov,[o] P. Tipton,[z] J.A. Valls Ferrer,[x] R. Van Berg,[u] V.I. Vassilakopoulos,[j] L. Vassilieva,[o] P. Wagner,[u] R. Wall,[z] C. Wang,[g] D. Whittington,[k] H.H. Williams,[u] A. Zhelezko[p] and K. Zhukov[o]

[a] *Faculty of Sciences, Department of Physics, Bogazici University, TR - 80815 Bebek-Istanbul, Turkey*

[b] *Brookhaven National Laboratory, Physics Department, Bldg. 510A, Upton, NY 11973, United States of America*

[c] *CERN, CH - 1211 Geneva 23, Switzerland, Switzerland*

[d] *Niels Bohr Institute, University of Copenhagen, Blegdamsvej 17, DK - 2100 Kobenhavn 0, Denmark*

[e] *Faculty of Physics and Applied Computer Science of the AGH-University of Science and Technology, (FPACS, AGH-UST), al. Mickiewicza 30, PL-30059 Cracow, Poland*

[f] *The Henryk Niewodniczanski Institute of Nuclear Physics, Polish Academy of Sciences, ul. Radzikowskiego 152, PL - 31342 Krakow, Poland*

[g] *Duke University, Department of Physics, Durham, NC 27708, United States of America*

[h] *Universite de Geneve, Section de Physique, 24 rue Ernest Ansermet, CH - 1211 Geneve 4, Switzerland*

[i] *Laboratoire de Physique Subatomique et de Cosmologie, CNRS-IN2P3, Universite Joseph Fourier, INPG, 53 avenue des Martyrs, FR - 38026 Grenoble Cedex, France*

[j] *Hampton University, Department of Physics, Hampton, VA 23668, United States of America*

[k] *Indiana University, Department of Physics, Swain Hall West, Room 117, 727 East Third St., Bloomington, IN 47405-7105, United States of America*

[l] *Joint Institute for Nuclear Research, JINR Dubna, RU - 141 980 Moscow Region, Russia*

[m] *Lunds Universitet, Fysiska Institutionen, Box 118, SE - 221 00 Lund, Sweden*

[n] *INFN Milano and Università di Milano, Dipartimento di Fisica, via Celoria 16, IT - 20133 Milano, Italy*

[o] *P.N. Lebedev Institute of Physics, Academy of Sciences, Leninsky pr. 53, RU - 117 924 Moscow, Russia*

[p] *Moscow Engineering & Physics Institute (MEPhI), Kashirskoe Shosse 31, RU - 115409 Moscow, Russia*

[q] *Lomonosov Moscow State University, Skobeltsyn Institute of Nuclear Physics, RU - 119 992 Moscow Lenskie gory 1, Russia*

[r] *Max Planck Institut fuer Physik, Postfach 401212, Foehringer Ring 6, DE - 80805 Muenchen, Germany*

[s] *LAL, Univ. Paris-Sud, IN2P3/CNRS, Orsay, France*

[t] *Department of Physics, University of Oslo, Blindern, NO - 0316 Oslo 3, Norway*

[u] *University of Pennsylvania, Department of Physics & Astronomy, 209 S. 33rd Street, Philadelphia, PA 19104, United States of America*

[v] *Petersburg Nuclear Physics Institute, RU - 188 300 Gatchina, Russia*

2008 JINST 3 P02014

[w] *University of Pittsburgh, Department of Physics and Astronomy, 3941 O'Hara Street, Pittsburgh, PA 15260, United States of America*
[x] *Instituto de Física Corpuscular (IFIC), Centro Mixto UVEG-CSIC, Apdo. 22085, ES-46071 Valencia; Dept. Física At., Mol. y Nuclear, Univ. of Valencia and Instituto de Microelectrónica de Barcelona (IMB-CNM-CSIC), 08193 Bellaterra, Barcelona, Spain*
[y] *University of British Columbia, Dept of Physics, 6224 Agricultural Road, CA - Vancouver, B.C. V6T 1Z1, Canada*
[z] *Yale University, Department of Physics, PO Box 208121, New Haven CT, 06520-8121 , United States of America*
[1] *Currently at Gaziantep University, Turkey*
[2] *Currently at Dogus University, Istanbul*
[3] *Currently at University of California, Riverside*
E-mail: ogren@indiana.edu

ABSTRACT: The ATLAS TRT barrel is a tracking drift chamber using 52,544 individual tubular drift tubes. It is one part of the ATLAS Inner Detector, which consists of three sub-systems: the pixel detector spanning the radius range 4 to 20 cm, the semiconductor tracker (SCT) from 30 to 52 cm, and the transition radiation tracker (TRT) from 56 to 108 cm. The TRT barrel covers the central pseudo-rapidity region $|\eta| < 1$, while the TRT endcaps cover the forward and backward eta regions. These TRT systems provide a combination of continuous tracking with many measurements in individual drift tubes (or straws) and of electron identification based on transition radiation from fibers or foils interleaved between the straws themselves. This paper describes the recently-completed construction of the TRT Barrel detector, including the quality control procedures used in the fabrication of the detector.

KEYWORDS: Particle tracking detectors; Large detector systems for particle and astroparticle physics; Transition radiation detectors; Particle identification methods.

2008 JINST 3 P02014

*Corresponding author.
†Deceased

Contents

1. Introduction

The Transition Radiation Tracker (TRT) is one of the three sub-systems of the ATLAS Inner Detector [1, 2]. It is designed to operate in a 2 T solenoidal magnetic field at the design luminosity of

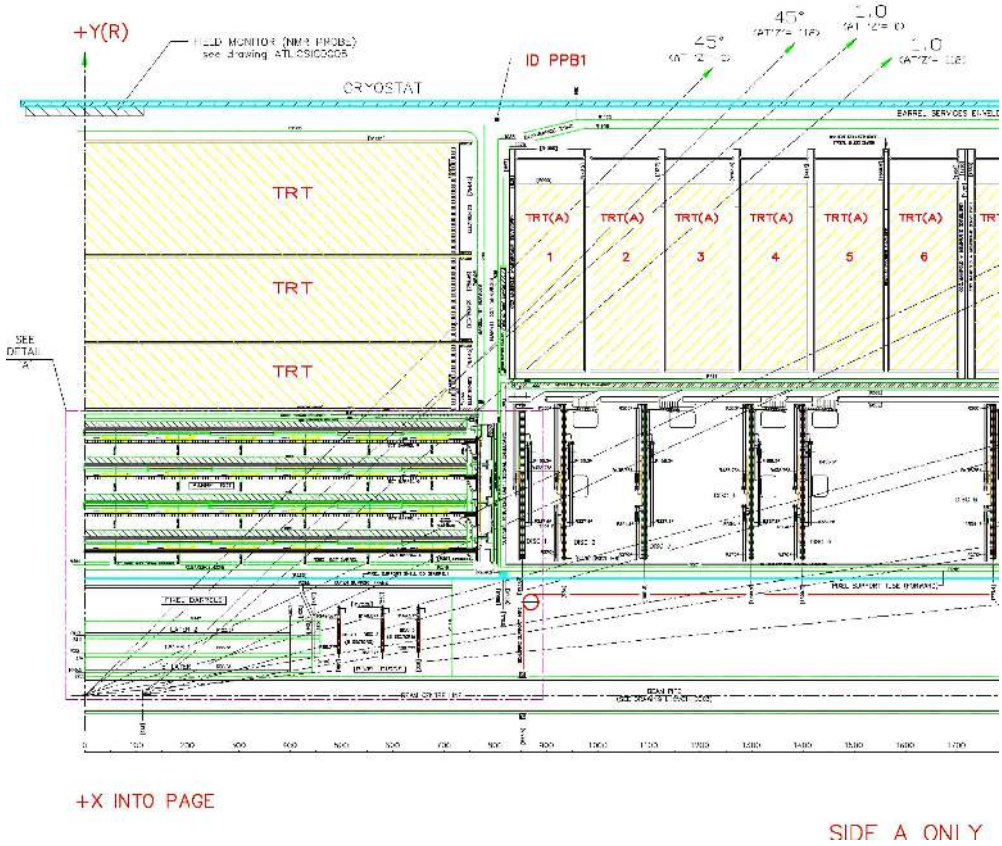

Figure 1. The ATLAS central tracker with the Pixel detector, SCT, and TRT. The Barrel TRT spans the Z region from 0 to 74 cm in this quadrant view. Part of the TRT endcap, SCT, and Pixel forward detectors can also be seen in the figure.

the CERN LHC, $L = 10^{34}\text{cm}^2\text{s}^{-1}$, in a very dense tracking environment with up to 10 events each 25-nanosecond crossing. A view of one quadrant of the Inner Detector is shown in figure 1.

The three main detector technologies of the inner tracker are shown in the figure, starting with the Pixel detector near the beam, then the SemiConductor Tracker (SCT), and finally the TRT occupying the outer region of the cryostat bore. The TRT section of the tracker is formed from a central TRT Barrel detector and a forward and backward TRT Endcap detector.The TRT Barrel provides continuous tracking in individual axial drift tubes (or straws), and of electron identification via transition radiation from fibers interleaved between the straws themselves. The TRT straw layout is designed so that charged particle tracks with transverse momentum $p_T > 0.5$ GeV and with pseudo-rapidity $|\eta| < 2.0$ cross about 35 straws (except for the Barrel/End-cap transition region). The TRT Barrel covers the radius range $56 - 108\,\text{cm}$ and has a sensitive region of total length of $144\,\text{cm}$ along the beam direction, corresponding to a pseudo- rapidity range of $|\eta| < 1$. The full length of the combined inner tracker is more that 7 m, and the maximum cylindrical radius is 1.08 m.

This paper gives an overview of the construction of the TRT Barrel detector; the evolution of the design and testing has been described in previous documents [3 – 20].

2008 JINST 3 P02014

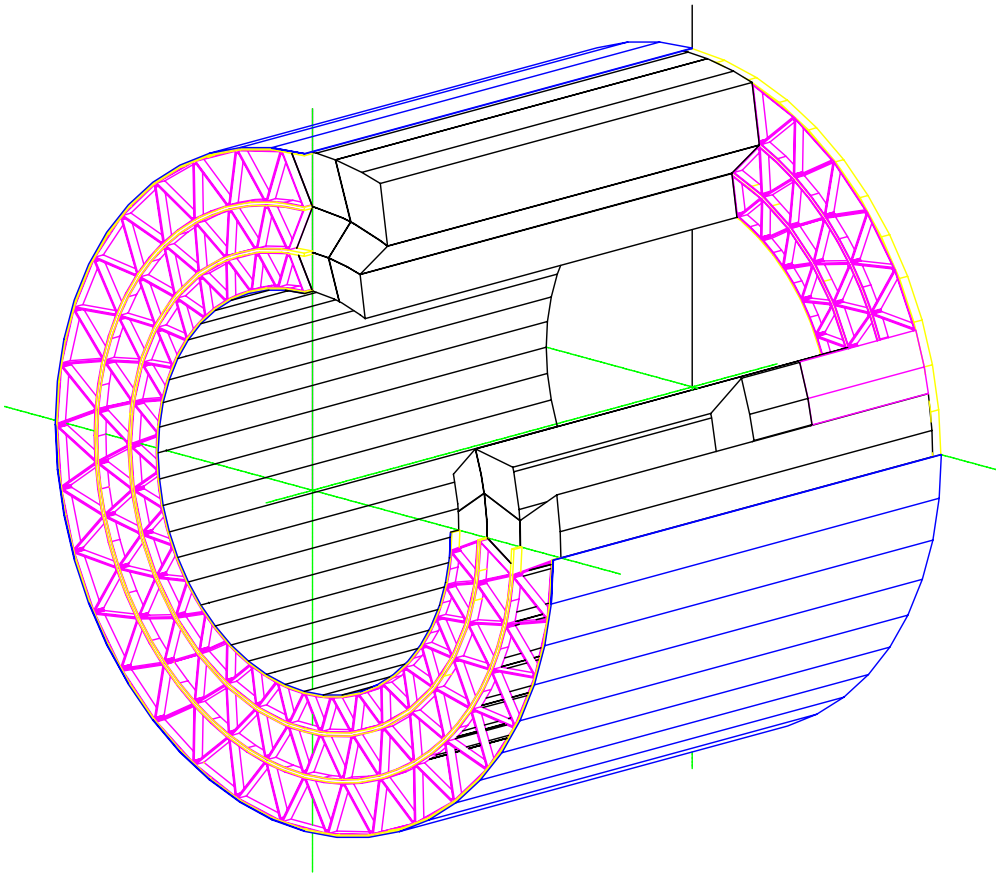

Figure 2. The TRT Barrel assembly, showing the Barrel Support System, in pink. The Barrel Support System supports and locates the two ends of each module.

2. TRT Barrel and component specification

The mechanical design of the TRT Barrel must satisfy many requirements, including the ability to operate at high luminosity with high reliability, and, high mechanical rigidity while maintaining dimensional stability with a minimum amount of material, plus, a reasonable level of manufacturability. Modularity has been used throughout the detector to simplify manufacturing and quality control, and to minimise at every stage the number of straws affected by any failure in the overall system. The TRT Barrel is divided into 96 modules of three types, arranged in three cylinders of 32 modules of each type, as shown in figure 2.

The modules are supported at each end by the Barrel Support System (BSS). Each module consists of a carbon-fiber composite cover or shell, an internal array of drift tubes, which are the detector elements, and an internal matrix of polypropylene fibers - the transition radiation material. The drift tubes (straws) were constructed from two layers of conductively-coated polyimide film. They form an approximately uniform array parallel to the beam axis, with an average spacing of about 6.6 mm between centers radially and tangentially. The layout of the drift tubes was designed to optimize the probability of the detection of transition radiation as well as to maximize the number of hits along a track. A more detailed description of the layout will be given when the straw positioning planes are discussed later.

2008 JINST 3 P02014

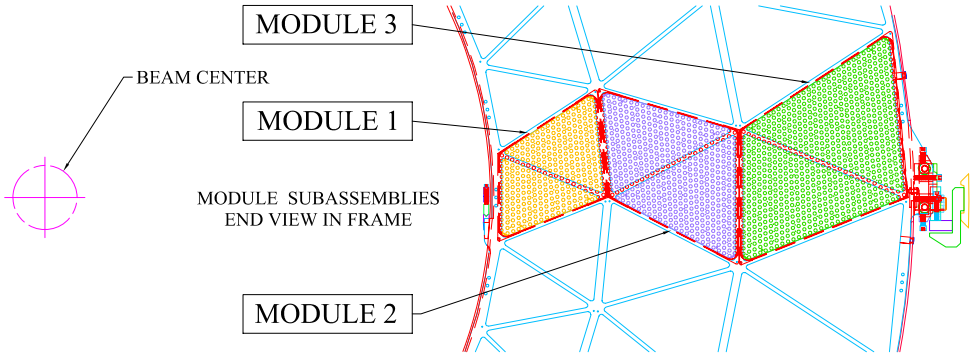

Figure 3. The three types of modules are mounted in the Barrel Support System. The orientation with respect to the beam intersection area is shown to scale. The triangular sections on the space frame are radially symmetric.

Table 1. TRT Barrel Module parameters.

Module	Inner Radius (m)	$\|\eta\|$ at Rmin	Layers	# Straws	Mass (kg)
Type 1	0.56	1.06	19	329	2.97
Type 2	0.70	0.89	24	520	4.21
Type 3	0.86	0.75	30	793	6.53
Total for Barrel			73	52544	439

A triplet of modules comprising a stack in azimuthal angle ("phi") is shown in figure 3.

The three sizes of Barrel modules are sequentially mounted in 32 "phi" sectors. Each module is a quadralateral prism with front and back faces in a plane perpendicular to the local radial ray, and sides that follow the close packing array shape of straws, approximating a 30° deviation with respect to a radial line. This design was choosen to minimize the amount of dead tracking area for high momentum particles. The resulting numbers of straws in each module are listed in table 1. The mass listed in the table are for modules only, with no electronics or external services connected. The total number of straws for all 32 sectors, and the total mass of the 96 modules is indicated in the bottom line of the table.

The straw diameter was chosen to be 4 mm as a reasonable compromise between speed of response, number of ionisation clusters, and mechanical and operational stability. The straw anodes are 31 μm-diameter gold-plated tungsten wires at ground potential and the straw cathodes are typically operated at a high voltage of 1530V, corresponding to a gas gain of 2.5×10^4 for the gas mixture chosen, which contains 70% Xe, 27% CO_2, and 3% O_2. To accomodate the high occupancy rate at the design luminosity, the sense wires are split in half by an insulating glass wire joint and instrumented with signal readout at both ends. The nine inner most layers are further divided into three sections with the middle section desensitized to further reduce the rate. The design and performance of the straw is described in detail in other documents [6, 21, 22], as is the evolution of the active gas mixture [14].

The dimensional specifications on the TRT were set by the requirements for the tracking precision to be optimized for the drift tube straw intrinsic resolution of 130 μm. Multiple measurements

2008 JINST 3 P02014

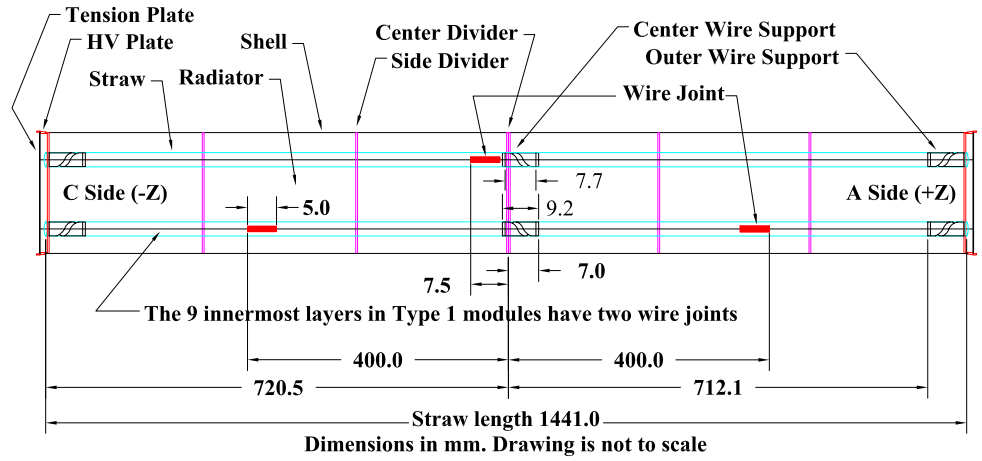

(a) Barrel module layout showing straw components and wire joint positions. Active sense wire regions can be calculated from the dimensions given. The upper straw shows a wire with single wire joint. The lower straw shows a wire with two wire joints.

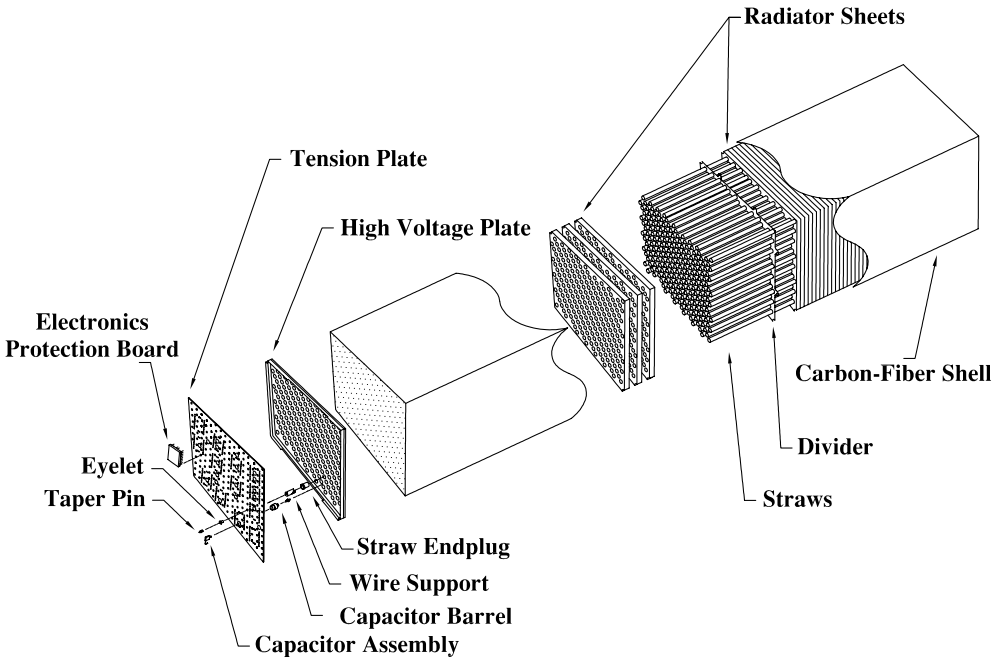

(b) Isometric view of a module with end plates, radiator, straws and shell.

Figure 4. Layout of a Barrel module.

in each module linking through the three module layers required that the position (radially and tangentially) of each straw in a module be precise to $\pm 40\,\mu$m, and the position of each module end to $\pm 50\,\mu$m. All mechanical components were constructed to satisfy these global specifications.

Figure 4 illustrates the layout of a Barrel module. The Barrel components will be discussed in subsequent sections.

2008 JINST 3 P02014

2.1 Barrel Support System

The Barrel Support System (BSS) is the key structural component of the Inner detector assembly. It is comprised of two endframes connected together by an inner and outer cylinder. The BSS itself is supported on rails mounted to the inside of the ATLAS Liquid Argon Cryosat. It is shown in figure 2. The three layers of TRT barrel modules are supported at each end by the endframes of the BSS, and in addition the SCT barrel structure is supported by rails attached to the inside of the BSS inner cylinder.

The BSS is required to have minimal temperature related distortion, and maximal strength and stiffness since it determines the alignment of both the TRT barrel modules as well as the SCT. These constraints were satisfied, as well as restrictions on the mass and radiation length, by building the structure from carbon composites. The extensive performance requirements are given in CERN Technical Specification documents [42, 43].

The open strut system of the endframes was constructed from a large carbon fiber laminate disk, 21 mm thick, that was machined to produce the 2 meter diameter triangular strut array.The strut system permits access to the ends of each module, while at the same time giving high structural stability. The 3 mm diameter module mounting holes on the endframes (two for each module end) were machined to within $50\,\mu$m position tolerance from the hole's specified position across the 2 m face. The two endframes are glued to a 2 mm thick continuous carbon fiber laminate cylinder at the inner radius forming the "spool" shown in figure 5. The BSS was manufactured in Russia [23].

Individual modules were inserted from the outer radius and were held at each end by two steel pins that pass through the precision drilled holes in the BSS and engaged a hole and a slot machined at two opposite corners of each module end assembly. After module insertion, two 3 mm thick carbon fiber laminate half cylinders were attached on the outside radius. The struts and cylinders were covered by copper foil to increase the conductivity of the carbon fiber to form a Faraday shield.

2.2 Shell specification and acceptance

The module shells were designed to minimize the thickness (and mass) of material while restricting the gravitational sag to less than $40\,\mu m$ in any module supported only at the ends. The module-to-module shell separation was kept less than 1 mm, to avoid compromising the uniformity of the array of tracking points. The module shell also acts as a gas manifold for the flow of gas (CO_2) that flushes the outside of the straw drift tubes and ensures that the ionization gas mixture, containing xenon, does not accumulate outside the straws through small leaks or diffusion. The flushing gas also ensures that we have a dry, high voltage insulating, gas outside the straws. This flushing gas enters at one end of the type-1 modules and passes serially through a "phi" stack of modules exiting at the opposite end of a type-3 module.

A module shell with the required $400\,\mu$m wall thickness was produced in by a carbon composites manufacturer in California [24]. It was shown to satisfy the deflection requirements of a maximum of $40\,\mu$m sagitta sag under full load in any orientation. The required flatness for the shell walls was $250\,\mu$m. The design of the shell was based on 8 layers (90,+45,0,-45,-45,0,+45,90) of XN50A carbon fiber in a balanced, symmetric layup using RS12 resin. This fiber was chosen

2008 JINST 3 P02014

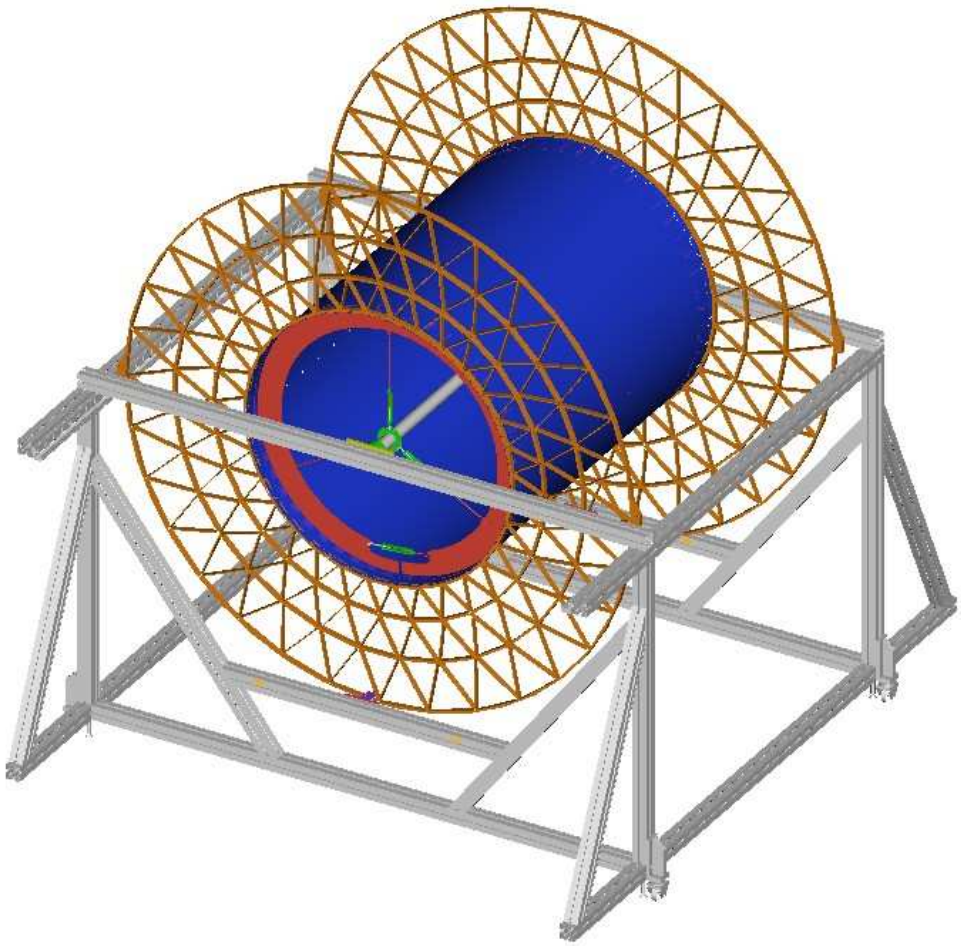

Figure 5. Barrel Support System without the outer cylinder halves which was attached after the modules were installed.

for the very high thermal conductivity ($200\,\mathrm{W/(m\cdot K)}$) since the module shells are cooled along two edges, and must provide an approximately isothermal package.

At full LHC rates, the average ionization current generates significant heat in the gas. The heat generated is directly proportional to the straw counting rate and is estimated to be as high as $10-20$ mW per straw at LHC design luminosity. To satisfy the basic requirements on straw operation stability and gas-gain uniformity, the temperature gradient along each straw should not exceed $10\,^{\circ}\mathrm{C}$. To meet this specification and to remove the heat, Fluorinert$^{\mathrm{TM}}$ liquid is used to cool the modules (and the front-end electronics). The liquid is passed through cooling pipes in the acute corners of each module in order to maintain the Barrel-module shells at an approximately constant temperature. A thin-walled Kapton® tube was glued in the two inside corners to hold the cooling line in close contact to the wall. The thermal conductivity of the shell material was measured to be $57\,\mathrm{W/(m\cdot K)}$. With the present shell material and the properties of the radiator, the internal temperature rise at full luminosity is calculated to be less than $5\,^{\circ}\mathrm{C}$ above the temperature of the cooling tubes. The calculation has been verified in a 0.5 m long prototype module [21].

The module shells were produced by hand lay up of the fiber material on three different sized

aluminum mandrels. A 50 μm Kapton layer was bonded into the module as the first layer on the layup. This was used for ensuring gas tightness and HV insulation between the shell and the straws which are at high volage. Upon receipt at our assembly sites the shells were checked for overall dimensions and thickness. The shells were cut to length (1444 mm) and penetration holes for the straw alignment planes were machined in the sides.

The modules were scanned with a touch probe device on a granite table to verify overall straightness and out-of-plane side panel deviations. All the shell edges near the corner at each side of the module were required to be within a specification of $\pm 200\,\mu$m along the full length. The flatness requirement was that the module sides (which are much less stiff) were required to be extend no more than 500 μm from nominal, which is the stay clear distance for each module. The average module shell weights were 570 g, 712 g, 892 g for types 1, 2, and 3 respectively.

2.3 Straw alignment plane (divider) specification and acceptance

The wire offset with respect to the center of each straw drift tube must not exceed 300 μm for stable operation at the LHC. The maximum wire gravitational sag at wire tension of 70 grams-force is $< 15\,\mu$m, so the allowed offset is actually a specification on the straightness of each straw. In order to meet this centering requirement, the straw straightness must be maintained over the full length of the Barrel module to less than 300 μm. It is the shell stiffness that provides, via the straw alignment planes, the necessary alignment of the straws, given that the gravitational sag of a fully loaded carbon-fiber shell has been measured to be $< 40\,\mu$m in any orientation.

Five alignment planes are positioned 25 cm apart along the module. Each plane has a straw-locating main sheet with two tabs on each edge (figure 6). The tabs pass through slots in the shell and holes in the tabs are held on an external alignment frame, and then glued to the shell. The aligment planes also function to maintain the shell wall profile under all loads, and so to strengthen them. To make assembly easier, each divider is sandwiched with two or three sheets of 100 μm thick Ultem® film glued to one or two polystyrene foam spacers. Each sheet has an appropriaxte pattern of holes; the main sheet in each divider has holes 4.3 mm in diameter and two alignment tabs on each edge. The other sheet or sheets are stiffeners with larger holes and no tabs. Four of the five alignment planes have a main plane, foam spacer, and one stiffener sheet. The central plane has a stiffener, foam spacer, main sheet, foam spacer, and second stiffener, for symmetry.

The Ultem sheets and foam parts were wet machined by a precision instrument manufacturer [25]. The perimeter features and the holes were wet machined in stacks of Ultem. Calibration testing had determined the expansion factor during wet machining for each type of sheet (~ 1.004). The machined sheets were washed and dried at an assembly site, and checked for dimensional correctness by measuring the 4 corner positions with a Zeiss optical coordinate measuring machine with 5 μm accuracy. The planes were then assembled at another assembly site.

Following assembly, each hole of each divider was inspected using a microscope to ensure that clearance was maintained and that the sheets were properly glued to the foam stiffeners.

2.4 Radiator specification and acceptance

The transition radiator material which completely surrounds the straws inside each module consists of polypropylene-polyethylene fiber mat about 3 mm thick [26]. This material had been chosen after

2008 JINST 3 P02014

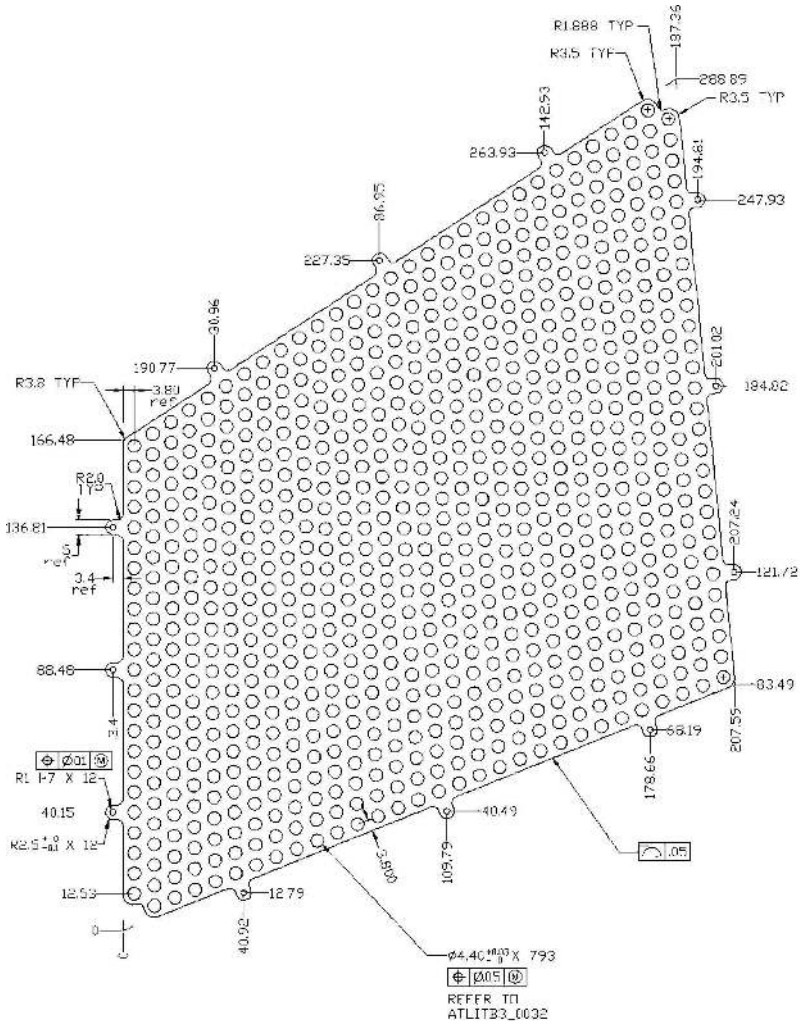

Figure 6. A straw alignment plane (divider). This figure shows a divider for the Type 2 module. The external tabs are for alignment only. They extend through small holes in the shell and are cut off after the divider is glued to the shell.

an extensive series of tests with prototype modules in CERN beam [2]. The fibers are typically 19 μm in diameter and are formed from polyethylene clad polypropylene material. The fibers are formed into fabric plies with 3 mm thickness and a density of about 0.06 g/cm^3. The absorption length for the lowest energy photons of interest (5 keV) is about 17 mm in the radiator material.

The fiber material was delivered as rolls 0.4 meter in width. The radiator fiber sheets were formed by stamping the pattern of straw holes into the fiber sheets. Three die sets that accurately cut the several hundred holes and the edges were produced. A production stamping company [27] punched the 50,000 fiber mats necessary for the TRT Barrel. A full-length module contains about 500 such pieces. The hole pattern is identical to that shown previously in figure 6 for the divider planes, except that the holes in the radiator material were 4.8 mm in diameter.

The radiators were produced over a period of two years by the stamping company. When a set

2008 JINST 3 P02014

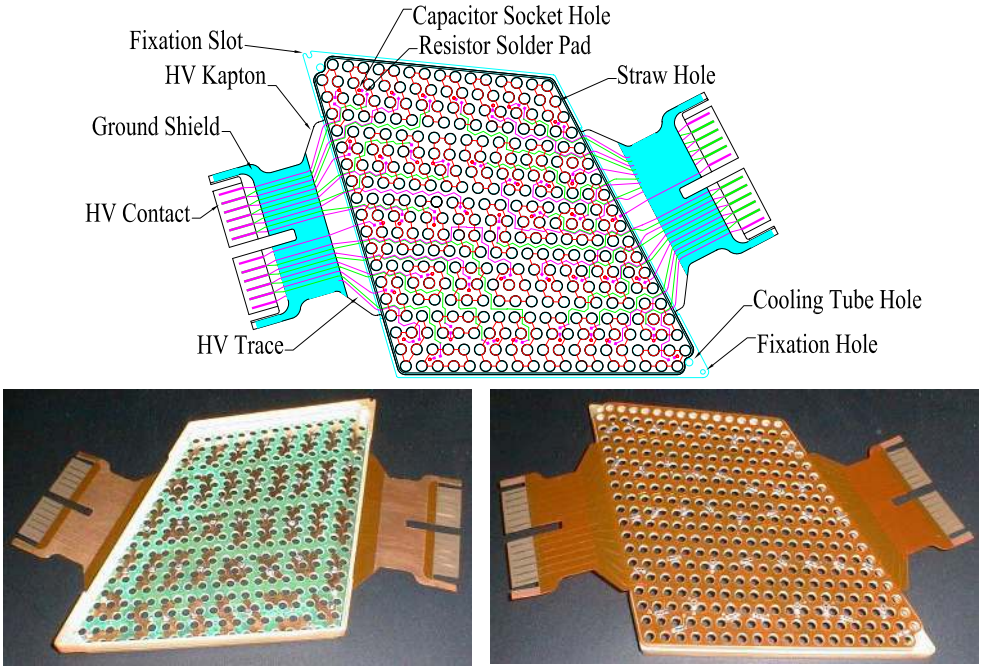

Figure 7. Upper plot is a transparent view of the HV plate showing HV circuits. Lower photos are front and back view of a HV plate before bending the HV Kaptons. In the left hand photo one sees the thin plate inserted into the well of the thick plate and in the right hand photo one sees the Kapton HV feed on the reverse side of the thick plate. Connection between the HV feed and the thin plate is made via the capacitor socket.

of radiators arrived, they were accompanied by a test stamping sheet, so that obvious errors could be spotted quickly.

The boxes of radiator, each containing a known number, were weighed and sorted by density. Due to variations in the manufacture of the fiber, storage and compaction, and handling during stamping, the density varied considerably. However, aligned bundles of mats were sorted and shuffled to produce more uniform density. These bundles were produced at one of our assembly sites and distributed to all sites for insertion into the modules during assembly. Each of the bundles fit between the divider plane sections. The average weight of the radiator in each module was 1.12 kg, 1.65 kg, 2.59 kg for types 1, 2, and 3 respectively, with a variation of $\sim 2\%$

2.5 HV plates

The high voltage (HV) plates bring high voltages from outside the module into the straw cathodes. They also play an important role mechanically for the module structure and alignment. Figure 7 shows a drawing and photos of an assembled HV plate. The HV plate is made of three main components as described below.

2.5.1 HV feed

The HV feed is a Kapton flex circuit [29] that plugs into the fuse boxes and carries high voltage on a number of copper traces embedded in between layers of Kapton. Each trace goes to a surface-mounted 4.7 kΩ, 2.0mm $\times$ 1.3mm size filter resistor and is then connected to a pad that accepts a

2008 JINST 3 P02014

socket for a capacitor to return cathode signal current to analog ground. The HV feed is made in three different layers. The center layer consists of 50 μm Kapton sheet with 35 μm rolled copper on each side. The two outer layers are 25 μm coversheets of Kapton with 25 μm acrylic bonding adhesive. The circuits were chemically etched on both sides of the center layer. Then, the part of each trace that will be in contact with the fuse boxes was selectively gold plated. No nickel or nickel flash were permitted before gold plating due to trace cracking problems that developed during bending of early versions.

2.5.2 Thick plate

The thick plate is a tray shaped FR-4 [30][1] structure precisely machined to mate between the tension plate and the shell and carries series of precision holes for mounting the module in the space frame, for holding the straws in their positions, and for the feed through of the module cooling tubes.

On the outer perimeter, the side facing toward the radiator must fit properly inside the module shell while the other end facing toward the space frame must be appropriately sized to not interfere with neighboring modules. The stated tolerance for outer perimeter dimensions is $+0.0$ mm and -0.10 mm per side.

The inner perimeter of the HV plate must allow clearance for the edge straws while simultaneously allowing clearance for the cooling tube holes which penetrate the HV plate at the acute corners just outside the inner perimeter. The stated tolerance for this inner perimeter's dimensions is ± 0.03 mm.The distance between the HV plate and the tension plate surfaces is 5 mm and must be controlled to provide proper clearances for mechanical and electronic components in between.

A major function of the HV plate is to locate each straw within the module. This is done by holes in the thick plate through which the straws pass. These holes, as well as the holes through the HV feeds and the thin plates (which are larger than the holes through the thick plate) must be aligned during assembly to allow subsequent insertion of the straws during module assembly.

The thick plate holes are located relative to the fixation pin holes/slots at the acute corners. These holes/slots fix the relationship between the modules and the attachment to the TRT Barrel Support System.

Table 2 lists the machining tolerance for the straw holes and the fixation holes/slots. The final precision on straw location requires that the deviation of the sense wire from the center of the straw shall not be more than 0.3 mm [1, 2]. An accumulation of tolerance limits the allowable circular variation of straw hole-positions relative to the fixation/alignment holes. The tolerances listed in table 2, combined with the twister, sleeve, end plug, and straw tolerances result in an expected variance of wire center position of 91 μm. This represents the part of the accumulated tolerance that can be allowed to HV plate assembly.

During production the thick plate hole positions were surveyed using a non-contact optical measuring machine [28] and compared to the theoretical values before they were assembled into HV plate.

[1] FR-4, an abbreviation for Flame Retardant 4, is a type of material used for making a printed circuit board, http://en.wikipedia.org/wiki/FR4.

2008 JINST 3 P02014

Table 2. HV plate machining tolerance.

Parts	Tolerance
Straw hole diameter	$+0.03\,\text{mm}/-0\,\text{mm}$
Straw hole position	0.075 mm radius
Fixation slot width	$+0.03\,\text{mm}/-0\,\text{mm}$
Fixation hole diameter	$+0.03\,\text{mm}/-0\,\text{mm}$
Fixation slot/hole position	$\pm 0.03\,\text{mm}$

2.5.3 Thin plate

The thin plate is a 0.2 mm thick single-sided FR-4 printed circuit [29] which carries pads that connect each group of eight or seven straws to each other and to a capacitor-socket hole. This hole is aligned with a hole in the thick plate and the capacitor-socket hole in the HV feed. A capacitor socket passes through all three pieces of the HV plate and is top and bottom soldered to connect traces on the HV feed to pads on the thin plate.

2.5.4 Assembly of the HV plate

The three parts of the HV plate, the HV feed, the thick plate and the thin plate are first glued with Araldite® 2011 epoxy. Then, the resistors are soldered to the HV feed, and the capacitor sockets are soldered to the thin plate and the Kapton circuit. The flaps of the HV feed are then bent 90° following the edge profile of the thick plate. This folding is done by heating and bending the Kapton on a 250°C heating block. The heating block is machined to match the edge profile of the HV plate. After bending to 90° the Kapton is clamped against the heating block to cool down. When the temperature reaches below 100°C, the clamp is opened and AY103 epoxy is applied between Kapton and the thick plate. The assembly is then clamped again and the epoxy is allowed to cure overnight as it gradually cools to room temperature. Electrical continuity is checked between the Kapton feed and the thin plate sockets to ensure no breakage during the bending process.

2.5.5 HV stability

The electrical stability of the HV plate is characterized by its leakage current, the micro-discharge rate and the breakdown voltage under high voltage.

The leakage current measurement is repeated several times from trace to trace and from trace to shield during module production, and is required to be $< 50\,\text{nA}$ at 3000V in dry air.

The micro discharge rate was sampled for a finished HV plate and was determined to be $< 0.01\,\text{Hz}$ at 5 pC threshold under 3000 V in dry Nitrogen.

Destructive breakdown voltage test was not carried out on finished HV plate, however, the HV plate operates at 3000 V in dry air without problem. Discharges sometimes occur due to contamination on the surface and can be eliminated by cleaning.

2.6 Tension plate

The tension plate is a 2-mm thick double-sided printed circuit board made of FR-4. It provides wire fixation mechanism using eyelets and taper pins, and, combined with the HV plate, forms a beam

2008 JINST 3 P02014

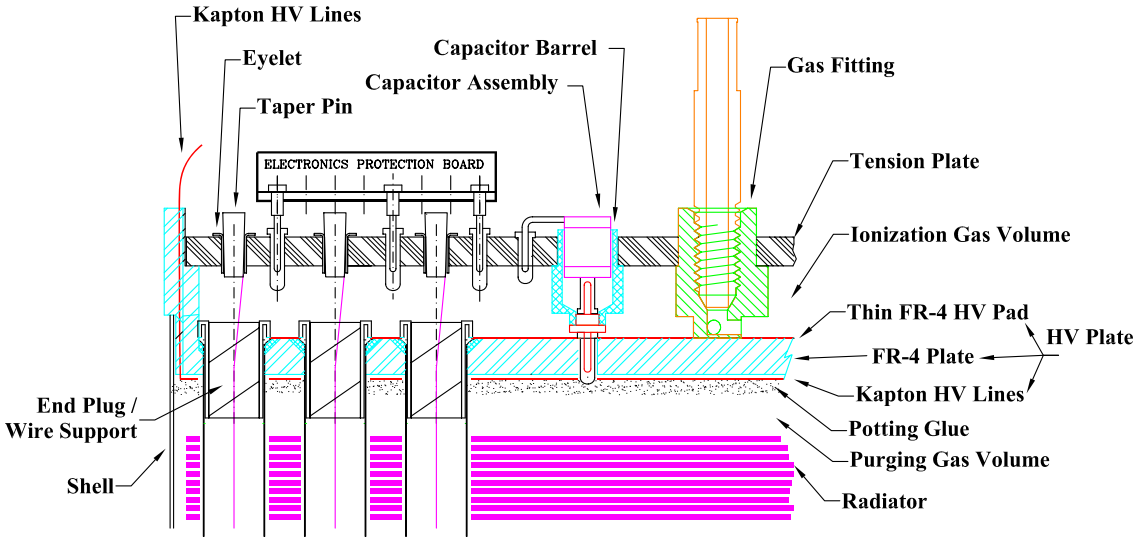

Figure 8. Tension plate and HV plate at module end.

structure that transfers wire tension to the carbon-fiber shell and the straws. In addition to taking the wire tension, the tension plate also serves as the interface between the module and the outside world. The empty space enclosed between the tension plate and the HV plate is a gas volume. This volume buffers the ionization gas from external pipelines into individual straws. The printed circuit traces on the inside of the tension plate brings signals from anode wires to an array of sockets on the tension plate. These sockets are where the external electronics is connected. The outer side of the printed circuit is a ground plane which provides signal return for the straws through HV blocking capacitors connected to the HV plate. The ground plane also serves as the analog ground for the external electronics [31]. Together with the shell, the tension plate is also part of a Faraday shield for the module. Figure 8 shows a cross section view of the tension plate region and its related components. The tension plate includes the following components:

2.6.1 Eyelets and taper pins

The eyelets are Stimpson stock item A1994 flat flange eyelets. The taper pins are custom machined part [33] to fit the eyelets, 3.43 mm long with a taper of 37 mm/m. Both eyelets and taper pins are made of brass and gold plated. A crimping mechanism is used to force the two brass pieces against the tungsten sense wire during stringing of the module. The back of the taper pin is machined with a blind hole. This is to reduce material and to facilitate handling and removal if needed. The diameter of the blind hole, 0.71 mm, is made to the tap size of a #1 screw so that a steel screw can be threaded into the taper pin and grab it for extraction.

2.6.2 Capacitors and capacitor barrels

The capacitor barrel provides a pocket between the tension plate and the HV plate that allows a capacitor to connect to the HV plate without disturbing the ionization gas volume. In the case of a capacitor failure, the capacitor can be replaced without having to open up the tension plate which would require cutting all the anode wires. The capacitor barrels, distributed across the tension plate

2008 JINST 3 P02014

surface, also serve as spacers to maintain distance between the two plates and transfer wire tension from tension plate to the HV plate. The capacitor barrel [33] is made of Ultem 1000 with a double-sided pin glued at the end for electrical connection. The double-sided pin is gold plated brass and designed to fit the sockets on the HV plate on one end and the sockets on the capacitor on the other end. Because the capacitor barrel is part of the ionization gas enclosure, each assembled piece was tested with 1.4 bar dry air and submerged in water for 5 sec. to check for their gas tightness.

The capacitor is 875 pF NPO/COG type in an 4.6mm $\times$ 3.0mm size package. A reduced length Mill-Max PGA socket is soldered on one end of the capacitor for connection to the double pin. A custom made bent pin is soldered on the other end for connection to the tension plate ground socket. Both sockets and tail pins are gold plated brass. To ensure reliability the capacitors have to withstand a burn-in at 2750V in dry air for 10 days. In this test, about 0.2% of the capacitors showed signs of breakdown and were rejected. The final capacitor assembly is coated with Hysol PC18M urethane coating to protect against contamination and humidity. The capacitors are not installed until the module is complete and ready for operation. After they are installed, a thin layer of AY 103 epoxy is applied over the opening of the capacitor barrel to add redundancy to the gas seal. This thin layer of epoxy can be removed with a small tip solder iron if it's necessary to replace a capacitor.

2.6.3 Ionization gas fitting

Each tension plate is equipped with four ionization gas fittings [33] near the four corners. The gas fittings are machined from Ultem 1000. The gas fitting seats on the HV plate and shoulders against the tension plate. The fitting is hollow and threaded on the tension plate end for adapting to external gas lines. Three openings in the gas fitting near the HV plate end, 120° angle apart, allow the gas to flow into the ionization gas volume uniformly. In normal operation, only one diagonal pair of fittings is used on a tension plate. The other 2 are sealed up as spares. On a module, the opposite pair of gas fittings are used on each side of the tension plate to force a more uniform gas flow through the straws.

2.6.4 Pre-assembly of tension plate

After the bare tension plate is made and cut into shape, the eyelets and sockets are soldered. When soldering the sockets, they are held by a mock up electronics board so that the socket arrays will fit for the electronics to plug in. The capacitor barrels and the gas fittings are then glued to the tension plate from the inner side. This glue is cured with a matching HV plate plugged into the capacitor barrel pins and the gas fittings seated to ensure that the glued components will fit their mating parts. After soldering and gluing, the components on the inner side of the tension plate are coated with a layer of sealing glue (AY 103) to ensure gas tightness. Figure 9 shows pictures of the various tension plate components.

2.7 Straw drift tube

The finished drift tube consists of a conducting 'straw' tube, sense wire supports at either end and the centre, plus the sense wire with an insulating joint, as described in the TDR [2], p. 653. Details of the design and the performance of the drift tube are described in a separate paper [22]. Mechanical assembly is described below.

2008 JINST 3 P02014

(a) Taper pin, eyelet, socket. (b) Capacitor barrel, capacitor. (c) Ionization gas fitting.

Figure 9. Tension plate components.

Figure 10. Wire support drawings and photos. In the photo: Left - a bare wire support (twister). Middle - embedded in a cylindrical sleeve as a centre wire support. Right - embedded in a flanged sleeve as an outer wire support.

2.7.1 Center and outer wire supports

The center and outer wire supports are designed to keep sense wires centred in the straw. The wire supports must not obstruct the flow of the ionisation gas going through the straw, and must allow installation or removal of the sense wire during module construction.

Wire supports consist of a twister [34] and a surrounding Ultem sleeve [35]. The twisters are cut from an Ultem rod with a machined helical groove [36]. The depth of the groove is 25 μm greater than the radius of the rod, forming a 50 μm diameter hole along the axis. The length of the twister is 7.7mm, a little over one pitch of a helix 6.88mm, so that the sense wire is constrained radially in all directions.

Figure 10 shows drawings and photographs of wire supports. The finished centre wire support is glued in a sleeve to provide an uniform surface for gluing to the inner straw wall. The outer wire support is embedded in a sleeve with a flange [33] to facilitate conductive gluing from the straw end to the HV pad on the HV plate.

2.7.2 Straw preparation and acceptance

Reinforced straws arrived at the U.S. preparation sites in batches from reinforcement sites at PNPI [37] and Dubna [38], sorted according to straightness; each straw was 1.65 m long. About 64,000 straws were processed.

2008 JINST 3 P02014

Figure 11. Glue dispenser in cut-away straw.

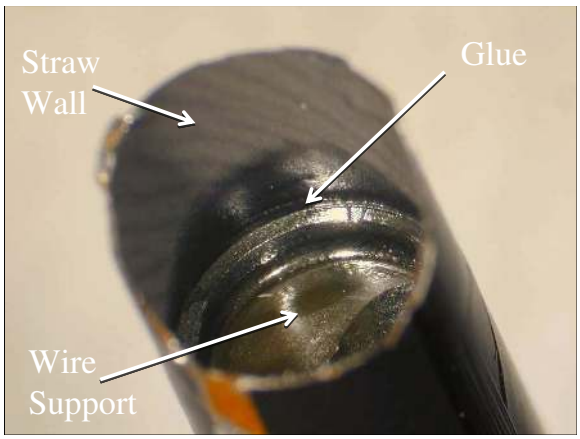

Figure 12. Center wire support in cut-away straw showing cured glue.

Since the centre wire support is not at the precise centre of the straw (it is offset from $|\eta| = 0$), each straw was first marked with a water-based latex paint at one end, to establish its orientation. Next, each straw was cut with scissors to a length of approximately 1.48 m, about 4 cm longer than the final length.

The next step was to glue in the centre wire support. This was done by batch in a jig. First, a drop of glue was placed by an glue dispenser at the centre of each straw. The dispenser was a glue reservoir at the end of a long stainless steel tube. Figure 11 shows the dispensing tip in a cut-away straw.

The glue-dispensing process required careful adjustment of tip distance from the straw, glue viscosity, air pressure, pressure pulse length, and speed of removal from the straw. Without correct adjustment, drops of glue can be left in the straw in the sensitive region. (This did occur in initial production, and led to the addition of a final quality assurance step: visual inspection of the interior.) Centre wire supports were then pushed down each straw over the glue drop (figure 12). After a short time the straws were removed from the jig and allowed to cure.

The next stage was to check the straws for leaks. This was done with an automated version of the leak-test system described in the TDR [2], p. 660. An elastomer seal was inserted into each end of the straw and expanded against the inside with a supporting collar on the outside. At one end, a central tube allowed the straw to be pressurized with dry air to about 5 mbar. After a short time to allow the gas to come to equilibrium, the pressure was measured over an interval of two minutes. If the pressure fell at rate corresponding to a leak rate of greater than 1 mbar/bar overpressure/min, the test was registered as failed. It would then be re-tested. A straw can be re-tested up to three times

2008 JINST 3 P02014

before it's rejected. Repeated tests were allowed because the sealing mechanism was imperfect: the interior winding of the straw created a spiral channel that could allow a leak. Overall, about 0.1% of straws failed this test, but that may have been due to seal failure, not straw leaks.

The design of the Barrel modules required that the straws were of a precise length: the end wire supports in each end of the straw had to contact the HV plate and not interfere with other components. The straw was cut to its final length, removing the part that had been in contact with the leak-test seal, in a cutting machine modelled after the one described in the TDR [2], p. 680. The production machine had rotating bypass shears made of tungsten carbide. The straw was mounted with a spacing rod inserted to position the centre wire support and the cylindrical internal 'blade' inserted into the ends. Clamps then held the straw in place while it was rotated so that the external blade cut the straw.

The length of every straw was assessed in a measurement jig using a digital dial gauge. The nominal straw length was 1441.00 ± 0.25 mm. Figure 13 shows the length assessments for about 65,200 straws, in terms of deviation from a nominal setting. The jig was set by indirect comparison with an Invar bar in combination with shims. One assembly site made and calibrated the Invar bars used by the other sites. A carbon-fiber rod with metal tips was then used to transfer the appropriate length from the bar to the measurement jig.

In addition to the length assessment, the position of the centre wire support was checked after the final cut.

The final step before packaging was interior inspection of the gluing side of the straw. This was done with an endoscope, about 2 mm in diameter, attached to a CCTV camera with the image displayed on a monitor. Straws with glue drops or other imperfections were rejected. Finally, the straws were packed in sealed polyethylene bags, with the batch bar code attached, and shipped to assembly sites.

2.8 Signal wire

The straw anode was a $31\,\mu$m gold-plated tungsten wire. This wire was produced by Toshiba at the Yokohama, Japan factory. The base wire material was pure (99.95%) tungsten with a density of $19.22\,\mathrm{g/cm^3}$ and was plated with pure gold. The thickness of deposited gold was $0.5\,\mu$m minimum to $0.7\,\mu$m. No nickel additives to the gold or nickel-flashing of the wire surface before gold plating were allowed.

Requirements on electrical stability for high rate operation, gas gain uniformity for Transition Radiation function, and radiation hardness for LHC environment imposed very stringent requirements on the quality of the wire and its production processes. The wire ellipticity corresponding to wire diameter variation was required to be less than $\pm 2\%$. The finished, gold-plated wire was required to have a tensile strength $700 - 800$ MPa.

The base wire had to be free of cracks, splits, or other defects. It was electrically polished to provide a smooth surface free from any pollutants and also carefully treated using light electrolytic cleaning to eliminate all traces of oxides and other possible pollutants immediately prior to gold plating.

The gold plating was required to be smooth, uniform and free of defects. Specifically, holes in the plating, poor adhesion, flaking, peeling, deep scratches, and blisters were not acceptable. The wire cleaning procedure following the gold plating process is critical. It ensured that the gold

2008 JINST 3 P02014

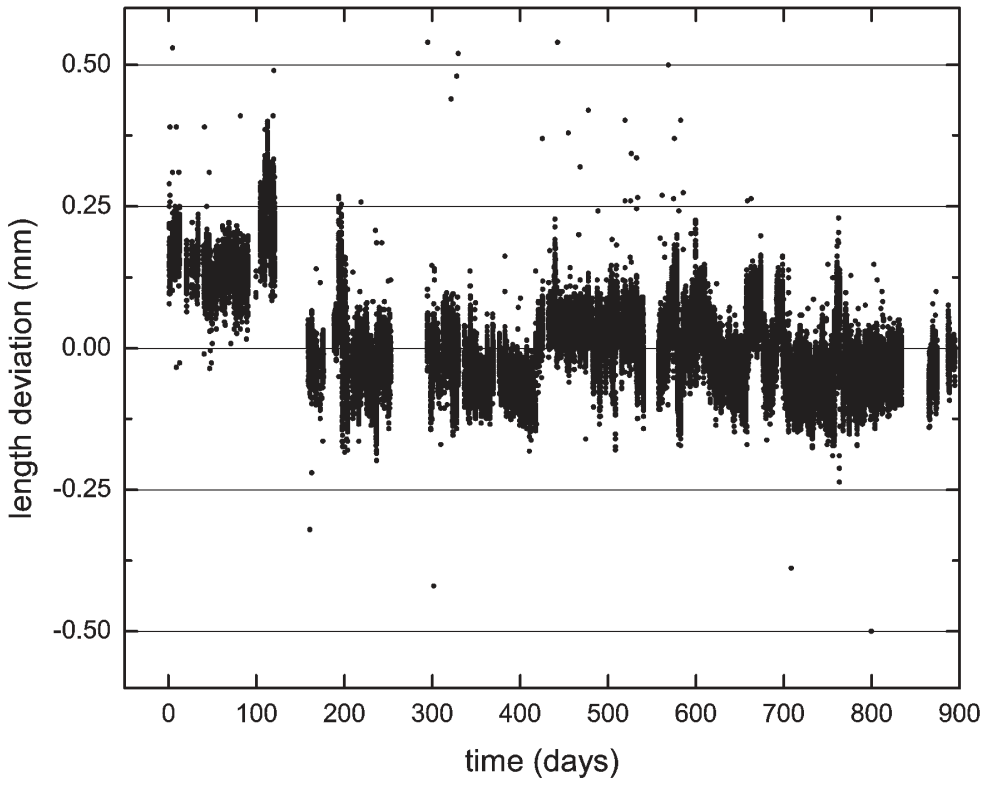

Figure 13. Straw length checks. The shift in the first 120 days is due to a mis-calibration of 0.15 mm.

surface is free from any chemical residue. No mechanical treatment of the wire surface was allowed after gold plating. This also implies special requirements for cleanliness and surface quality of all the parts of the set-up that are in contact with the gold plating surface during the gold plating process and the respooling process.

The wire was wound onto clean aluminium spools approximately: 95 mm ID $\times$110 mm OD $\times$20 mm height. Each spool typically held $3-4$ km of one continuous wire.

The wire was extensively inspected upon arrival using a scanning electron microscope (SEM) at North Carolina State University (Raleigh, NC). Typical images from these inspections are shown below in figure 14.

2.9 Wire joints

Due to the high occupancy of the straw tubes, especially at low R, it is necessary to split each sense wire into two electrically isolated wires, with each being read out from the corresponding end. To achieve this electical split, each sense wire consists of two wire sections joined by a length of glass tubing [39]. The pre-cut tubing, before any melting, is 6 mm long with an inside diameter

2008 JINST 3 P02014

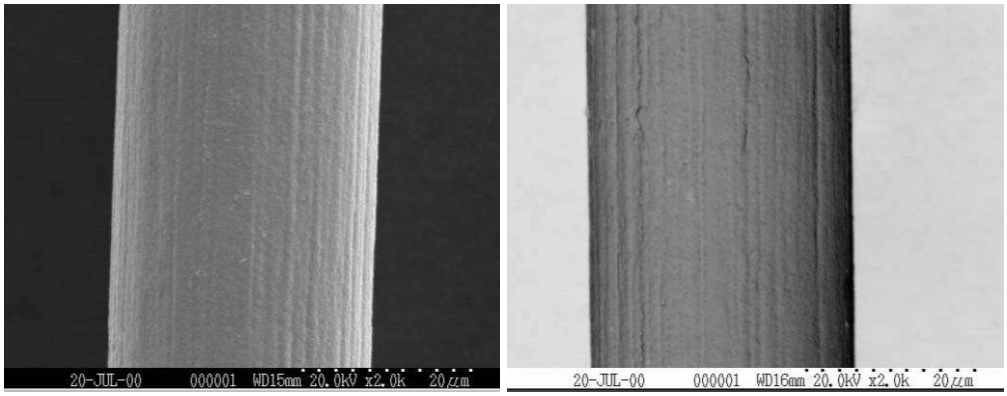

Figure 14. Two images of accepted gold plated tungten sense wire under electron microscope.

of 0.127 mm, and an outside diameter of 0.254 mm. The glass, Kimble EN-1® type, was chosen for its superior bond strength when fused to metal. The center 0.5 mm of each glass tube was first fused in a methane-oxygen flame to form a ball to prevent the subsequently inserted sense wires from becoming electrically connected and to aid in the alignment of the tube in the wire joint tooling. Each center-fused tube was inspected for completeness of melting and straightness. To make wire joints, the sense wire is unspooled and cut near the center of the wire joint jig. The glass tube is held in the jig and the cut ends are fully inserted until stopped by the fused center and then fused by a pair of flames into the tube. The wire is then taken up by a spool so that the next cut is made 2 m from the previous wire joint. This produces a continuous batch of sense wire with sufficient extra length to allow for handling during module stringing. The finished length of each wire joint is in the range $5.0 - 5.5$ mm. Each wire joint was visually inspected for completeness of melting, and periodically wire joints were tested by attaching to a force gauge and pulling to destruction. Properly made joints are stronger than the sense wire itself, so the wire breaks at 200 g of pull rather than pulling out of the tube or the glass breaking. This is ~ 3 times the maximum tension that the wires will have in the modules. For the straws at the smallest R, i.e. those in the first nine layers of each Type 1 module, the high occupancy requires that approximately the center third of the wire not being read out. For this case sense wires were produced with two joints per wire, spaced apart to create an 80 cm dead segment as shown in figure 4(a). Figure 15 shows a completed wire joint.

2.10 Preparation and acceptance of components

An important aspect of the manufacturing process was the shift from prototype methods to series production with consistent quality assurance procedures. To achieve a degree of uniformity, most or all of several kinds of components were prepared at a single facility at Hampton University and shipped to assembly sites at Duke University and Indiana University. These parts included straws, wire supports,dividers, shells, HV plates, tension plates, etc. A total of about 500,000 parts were processed, a database being used to track parts and batches, and to guide the preparation process — instructions for each procedure were presented to the technician on a screen and a response was required on the completion of each step. Bar codes on items or batches were recorded so that there was assurance that processing and assembly procedures were followed.

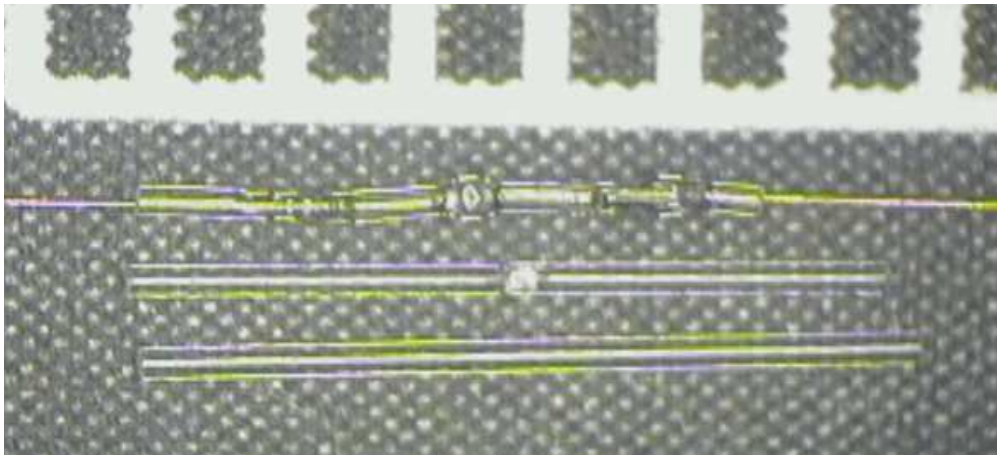

Figure 15. From the bottom up: a pre-cut glass tube, a center-fused glass tube, and, a glass wire joint fused to two sense wires. The fused center of the glass tube prevents the two wires from touching each other. White mark on top is a ruler in mm scale.

2.10.1 Common preparation processes

There were common features to the preparation of many parts particularly in cleaning and gluing.

Cleaning of small parts made of metal or Ultem (twisters, wire support sleeves, capacitor barrels, taper pins, etc.) was done via ultrasonic cleaning using a 2% solution of Micro-90 detergent in distilled water. Following this cleaning, the parts were rinsed in distilled water until the conductivity of rinse water was not distinguishable from that of distilled water. The parts were then dried in an oven at 110-120° C for 45 minutes, spread out on a tray in a single layer.

Assembly of composite parts (e.g., wire supports, dividers) was done with an appropriate epoxy. To speed up production, epoxy was set by baking the parts in suitable jigs for 1.5 hours at 60 to 65° C.

Specifications and quality control tests for small parts varied. For wire supports, samples from each batch were tested for adhesion of the twister to the sleeve by applying a longitudinal force; the glue joint had to support a load of more than 9 kg.

The brass taper pins were finish plated with 1.3 μm of 99.7% gold (130 Knoop hardness) over 2.5 μm of nickel, and over 2.5 μm of copper base plating. Quality control was by visual inspection of completeness of coverage. A similar specification was used for the tension plate eyelets.

3. Electronics and services

3.1 High voltage

High voltage is supplied to the TRT Barrel from power supplies in the electronics room through $\sim$ 100m of cables divided into 3 sections. The last section starts from the outer edge of the Barrel and distributes HV to the modules through sets of fuse boxes. Each fuse box is a two-half FR-4 shell enclosure containing filter circuits, fuses and spring contacts for direct connection to the HV feed in front of the modules.

2008 JINST 3 P02014

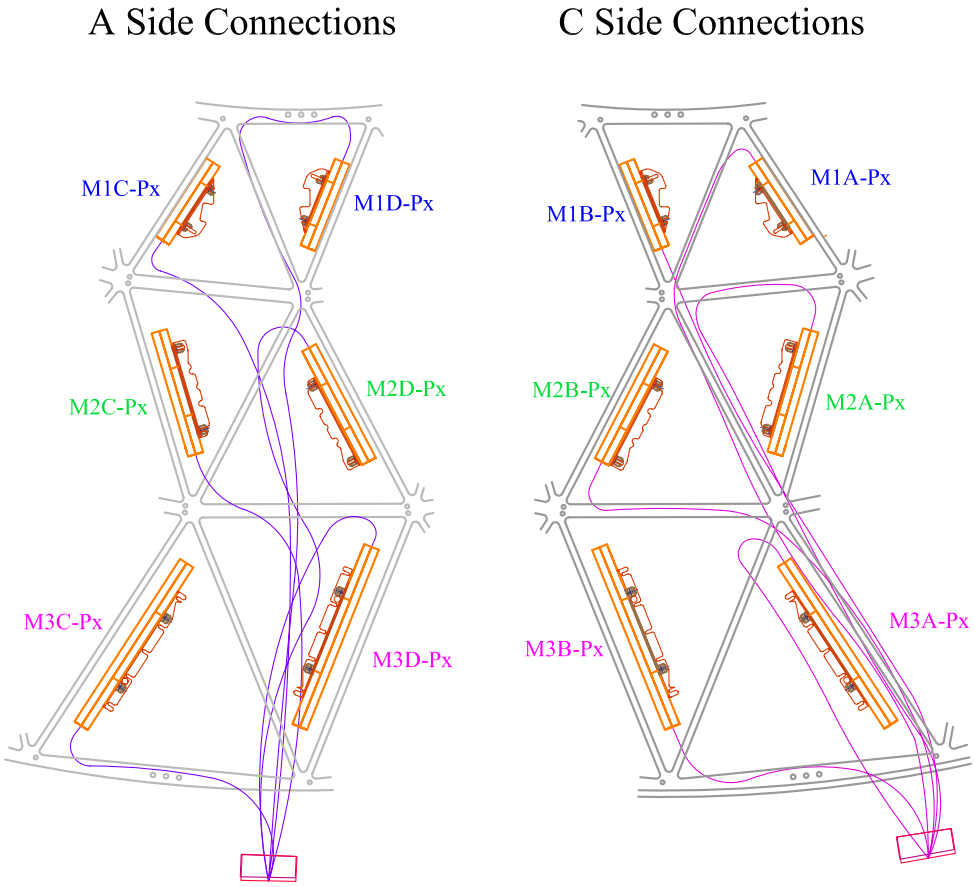

Figure 16. HV cable routing and fuse box connections to the modules. Six fuse boxes for 1 stack of 3 modules are bundled into 1 HV connector at the outer edge (bottom) of the Barrel.

A Barrel module has two HV feeds at each end to receive high voltage, however, fuse boxes and HV are only supplied to one end of the module. The two HV feeds on the other end are used as spare and protected by empty FR-4 dummy fuse boxes. Real and dummy fuse boxes alternate between neighboring modules and split HV lines equaly between the two ends of the Barrel. The wiring and fuse boxes are designed such that if one end of a module has a defect and is unable to receive HV, the other end can be used by swapping cables with its neighbors. Figure 16 shows fuse box connections on the modules.

3.1.1 Fuse box design and HV granularity

Inside each half of a fuse box is a 0.15mm thick double-sided printed circuit board glued on to the FR-4 casing and holding all the components as shown in figure 17. The HV mini coax cable entering the fuse box first goes through a filter circuit consisting of 1kΩ resistors on HV and return lines bridged by a 875 pF HV capacitor. The filtered return line then goes to a spring contact that will connect to the analog ground of the electronics. The HV line goes through fuses to the spring contacts that will connect to the module HV traces.

The fuses are 50kΩ and custom designed [40] to withstand occasional chamber discharges and

2008 JINST 3 P02014

power supply trips. When there is a broken sense wire and the fuse has to be disabled, a special HV pulse is injected from the power supply side to blow the fuse.

The nominal TRT operating voltage is 1530V. The fuse boxes are required to hold 2 kV with a leakage current less than 50 nA per HV line. After soldering and cleaning, they are baked and coated with urathane conformal coating to reduce surface leakage current.

The HV granularity is a trade off between cost, performance and tolerance in losses:

1. In order for the straw gas gain to be uniform across the Barrel, the voltage drop over the fuses and filter resistors due to current draw in the straws can not be more than 7 V at the design luminosity. This sets an upper limit on how many straws can be fed from a fuse or a HV line.

2. In case of a HV failure inside the detector, e.g. a broken sense wire, we want to minimize the number of straws that have to be shutdown by a fuse. This number is determined to be 8, and is implemented on the HV plate which groups 8 straws to share one trace on the HV Kapton.

3. To minimize the cost, a HV power supply should drive as many straws as possible up to a limit either set by the number of straws or the current draw. Based on the power supply specification, the nominal load assignment to a power supply is chosen not to exceed 1.5 mA, and, the maximum number of straws is chosen to be less than 100.

With these criteria, GEANT simulation was used to estimate current draw on each fuse at projected LHC luminosity. The fuses are then grouped to share HV power lines within the current limit. To simplify fuse box production and installation, symmetry is taken into account, and, the fuses are grouped such that one fuse box layout can be used on all 4 possible HV Kapton positions in a module. The results are 6 lines for a type 1 module, 6 lines for a type 2 module, and 10 lines for a type 3 module. The number of straws each line drives ranges from 48 in a type 1 module to 96 in a type 2 module. Type 3 module was assigned a uniform 80 straws per line for simplicity, despite its lower current draw [41]. The HV circuit and a picture of the layout with fuse grouping is shown in figure 17.

3.2 Electronics

The basic front end electronics [31] for the TRT Barrel is schematically the same as the electronics for the TRT End Cap - an ASDBLR (Amplifier, Shaper, Descriminator, Base Line Restorer) analog signal processing chip followed by a DTMROC (Drift Time Measurement Read Out Chip) time measuring.

The 8 channel ASDBLR ASIC in DMILL technology [32] performs the amplification, shaping and base line restoration. It includes two discriminators, one at low threshold for minimum ionizing signal detection and one at high threshold for transition radiation detection;

The 16 channel DTMROC in commercial 0.25m CMOS technology performs the drift time measurement (3 ns binning). It includes a digital pipeline for holding the data during the level 1 trigger latency, a derandomising buffer and a 40 Mbits/s serial interface using LVDS (Low Voltage Differential Signaling) for the readout. It also includes the necessary interface to the timing, trigger and control as well as DACs to set the ASDBLRs thresholds and test pulse circuitry for mimicking analog inputs to the ASDBLRs. These ASICs are housed on front-end boards attached to the detector. Details of this electronics can be found in the TRT electronics publication [31].

2008 JINST 3 P02014

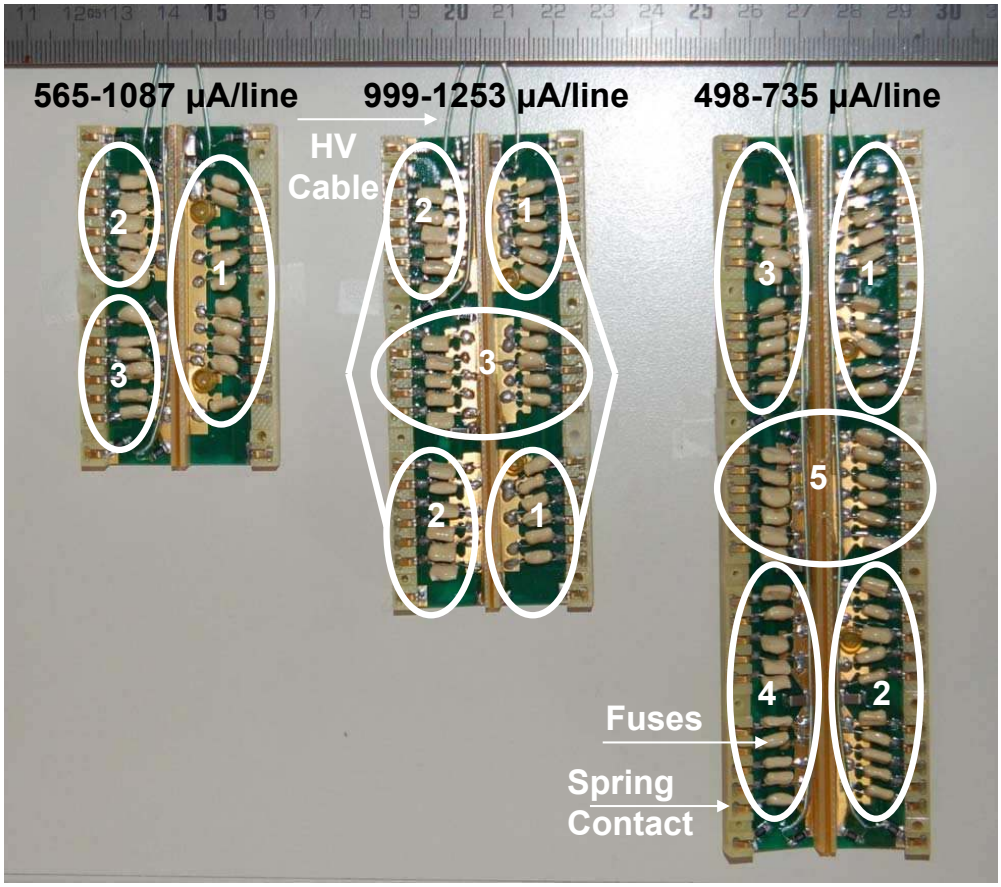

(a) The fuse box layout for module types 1, 2, and 3 from left to right with fuse grouping indicated in white and current draw ranges in black.

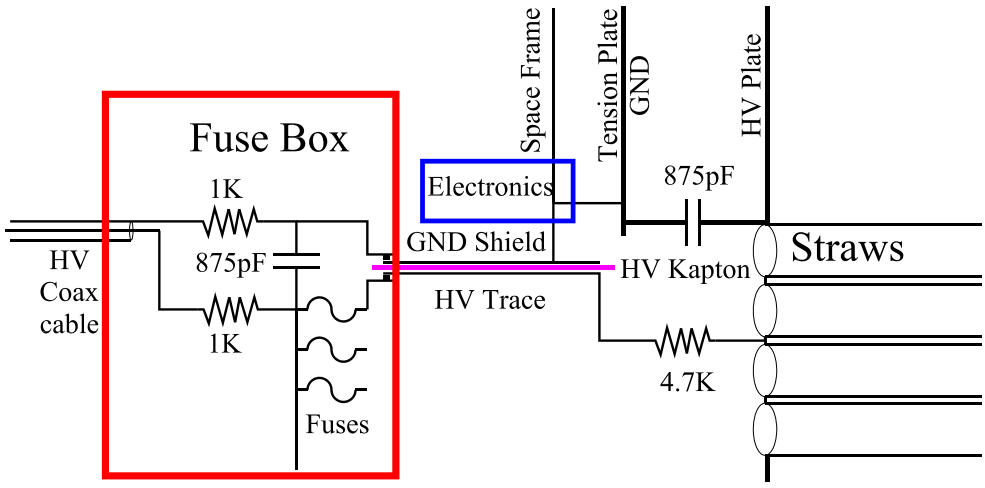

(b) Schematics showing HV circuit.

Figure 17. Fuse box and HV circuit layout.

3.2.1 Protection boards

Physical connections of the anode wires and the tension plate ground reference to the front end electronics is made via a small 22 pin "protection board". Each protection board connects 16 anodes and 6 signal returns using 0.5 mm diameter gold plated brass pins in a common physical pattern repeated across the faces of the modules. The corner pins for each protection board have PEEK[2] standoffs to ensure a common mating height for all the protection boards on a module. The outer surface of each protection board has a miniature 50 pin connector for connection to the front end electronics boards. The 50 pin connector has enough contacts to allow each anode signal to be accompanied by a "dummy" signal from the protection board up to the front end and the ASDBLR inputs and for each pair of anode and dummy to be separated by a signal return trace. The remaining surface area on both sides of the protection board is used to mount a limiting resistor (24 Ohms) and a clamp diode for each anode signal to provide additional protection for the ASDBLR inputs against electrical discharge.

The other function of the protection boards is to allow a mechanical degree of freedom for attaching the front end boards to the modules - even the smallest of the front end boards has ten protection boards, 220 brass pins that would be difficult to insert simultaneously and the largest front end board has 594 pins. The 50 pin connectors themselves provide some 300 microns of mechanical compliance which adds to the degrees of freedom for each individual protection board and yields a mechanical system that allows a surprisingly easy and reliable manual insertion of up to 1350 individual connections between the largest front end board and its ensemble of protecion boards.

3.2.2 Front end boards

The front end electronics for the TRT Barrel has physical and thermal constraints that are tighter than those for the Endcaps, thus the Barrel final front end board designs turned out to be significantly more challenging. Instead of a two board design for the Endcaps which allows some physical separation of the ASDBLR analog and DTMROC digital circuitry, both chips were combined on a single physical triangular substrate. More details can be found in [31].

The readout is segmented in 32 stacks in “phi” to ease the level 2 trigger task of data retrieval. The readout uses 40 Mbits/s electrical LVDS links to patch panel boards (PP2) located up to 13 meters away just after the first muon chambers. Further details about the back end electrlnics and the off-detector DAQ can be found in [31].

3.3 Cooling plates

The electronics as well as the modules themselves need to have heat removed from the detector area. This is accomplished by circulating C_6F_{14} (Fluorinert) from a central cooling plant to four distribution racks located near the detector and through the modules in the detector. For the design and tests of the cooling system it has been assumed, with enough of safety margin, that FE electronics generates 100 mW/channel. This heat is removed by conduction from surface of the DTMROC chip directly to an aluminum cooling plate attached to each of the electronic roof boards. The Fluorinert is carried by a cooling manifold from the outside radius of the BSS to the modules. In

[2]PEEK, Polyetheretherketone, is a thermoplastic with extraordinary mechanical properties, http://en.wikipedia.org/wiki/PEEK.

Figure 18. Exploded View of Cooling plate.

order to cool the modules themselves, which can produce up to 6 W/module at highest luminosity, the Fluorinert exits each cooling plate and passes along the length of the module to the opposite end before being carried away by a manifold to the outer radius of the BSS and ultimately back to the pumping station. There is a module cooling tube inside the shell in each of the acute corners of every module. This module cooling tube is made of 3mm PEEK and is connected to the electronic cooling plate at one end, and exits via the manifold at the other end. The nominal entrance temperature of the fluid is 15 °C, and the fluid flow is set to have a maximum temperature increase of less than 8 °C at the return.The cooling plate itself is shown in figure 18.

The cooling plate is made from two triangles of aluminum with aluminum input and output connections. All components are bonded with epoxy - Epibond 420. The top plate is machined to produce a path for the cooling fluid directed over the tops of the electronic chips. For increased protection against de-laminating, the two plates are riveted in numerous places as well as being glued. All plates were tested for tightness at 10 bar. The nominal operating pressure is about 3 bar.

The specifications for leak tightness was < 100 l/year for the entire manifold and plumbing system. The leak rate in any cooling plate was too low to measure, it was expected that the major loss would be in the interconnects of the manifold and plumbing connections. The cooling plates and manifolds have a total volume of about 3 liters while the plumbing ditribution lines from the racks in the cavern is more than 200 l. The coolant flows are 0.6 l/min for a type 3 module and 0.5 l/min for type 1 and type 2 modules.

3.4 Active gas, flushing gas and manifolds

3.4.1 Active gas

The active gas for the straw drift tubes is Xe(70%), CO_2(27%), O_2(3%). This gas is supplied through two ports at one end of each module, and exits from two ports on the other end of each

2008 JINST 3 P02014

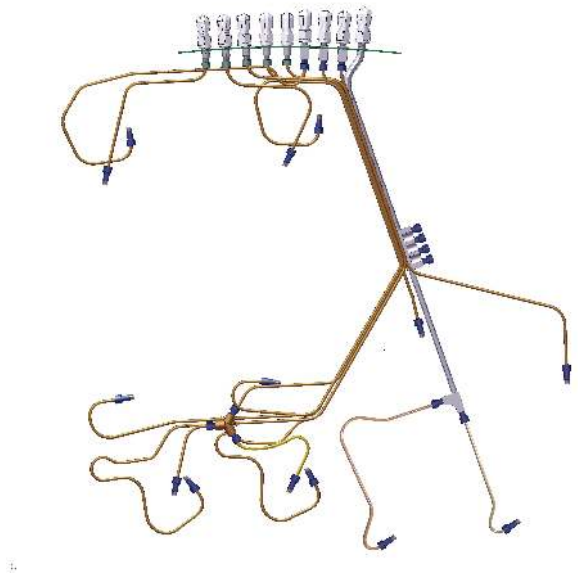

Figure 19. The cooling and active gas manifold for an 1/16 "phi" section. Active gas (five leftmost fittings) and cooling fluid (the next four fittings on the right) are supplied from the large radius fittings and distributed to the three layers of modules.

module. The gas volume within the module itself is the volume between the tension plate and the HV plate and the straws themselves. For the three module types the nominal flow rate is 110 cc/min for type 1, 170 cc/min for type 2, and 240 cc/min for type 3, which results in about one volume change per hour. The exit gas is recovered, cleaned and recirculated.

3.4.2 Barrel manifold

At each end of the Barrel there is a PEEK based manifold that carries active gas to each module. For the innermost modules (type 1) one manifold line feeds two modules in parallel. The active gas lines are part of the Barrel manifold shown in figure 19. The active gas and cooling manifolds are physically grouped into a radial network that links the supply line at the outer BSS radius to the individual modules.

3.4.3 Flushing gas

In the TRT Barrel the individual drift straws are separated by several millimeters. In between the straws there is the TR radiator. It is very important that Xe does not fill this region, otherwise the transition radiation photons would deposit their energy outside the straws. In order to sweep away any small amount of active gas that might have leaked or diffused from the straw wall, the radiator region is flushed with CO_2. The shell of the module has access holes that act as the manifold for this gas volume. The CO_2 gas flows at a rate of about 500 cc/min per stack of 3 modules. The gas enters at the inner radius of the innermost module, flows the length of this module and exits via a gasket coupling to the inner side of the middle module. Again it flows the length of the middle module and exits into the inner side of the outer most module, passing along its length and exiting at the outer radii. This is done for each of the 32 module stacks in "phi". The entrance end for

the gas flow alternates between "phi" stacks. The connection to the input coupling is made via a flexible PEEK tube that starts at the outer radius of the BSS (not shown in figure 19).

4. Assembly of modules

The assembly of a module is divided into two main parts, a "mechanical assembly" that puts together aforementioned parts to form the structural body of a module, and, wire stringing. In either process QA procedures are embedded wherever possible to ensure that the assembly is done correctly. The following sections describe the assembly processes in the sequence they occur. Module production began in the Fall of 1999 and was completed in 2004.

4.1 Alignment of straws

The assembly process starts with checking the alignment components of a module. The components that maintain the straw positioning in the module, including the shell, the two HV plates and the five alignment sheets are placed in an "assembly frame". The assembly frame is a portable support structure made of precision machined stainless steel rods and aluminum plates to hold a module by its alignment components through out the assembly processes. The assembly frame allows transportation of a module before its completion. However, for most critical tasks the assembly frame is mounted on calibrated stands on an optical table to achieve repeatable alignment requirements.

For checking the alignment components, nine fiducial straws in a 3x3 array are inserted in pre-defined locations. A laser aligned to the module axis is mounted on one end of the assembly frame and shines onto a target that slides inside the fiducial straw. The target is connected to a CCD camera through optical fibers from the other end of the assembly frame. The CCD image is read into a PC every 5 cm and analyzed for straw straightness profile. Figure 20 shows the setup and a typical module data. The measured deviation of the fiducial straw is a combination of deviations from the module components being evaluated, the assembly frame, the fiducial straws and the precision of the measurement method itself of 75 μm. In this test we require the combined deviation to fall within an envelope of $\pm 180\,\mu$m.

4.2 Radiator insertion

After checking the alignment components, the HV plates are removed and replaced by an aluminum rim to hold the shell. Four of the five alignment sheets, except the middle one, are also removed to allow insertion of radiator from each end of the module. Radiator sheets are pre-packed into blocks for each section between alignment sheets, and inserted section by section with alignment sheets restored in between. In order to keep the straw holes aligned across radiator packs, nine stainless steel tubes, replacing the fiducial straws, are used to guide the radiator packs as they slide in. These rods stay in place until they are replaced by straws.

After radiator packs are installed, the two HV plates are also re-inserted and tested with 3000 V relative to the shell to check for any defect in Kapton insulation.

2008 JINST 3 P02014

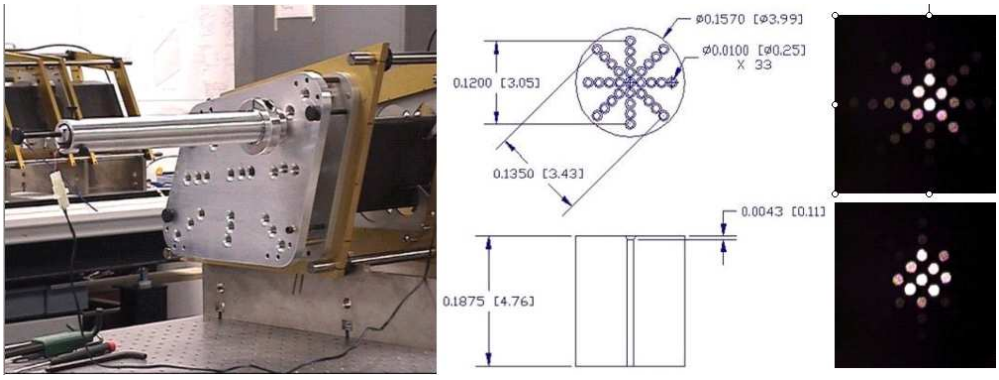

(a) Setup of the laser system and the target.

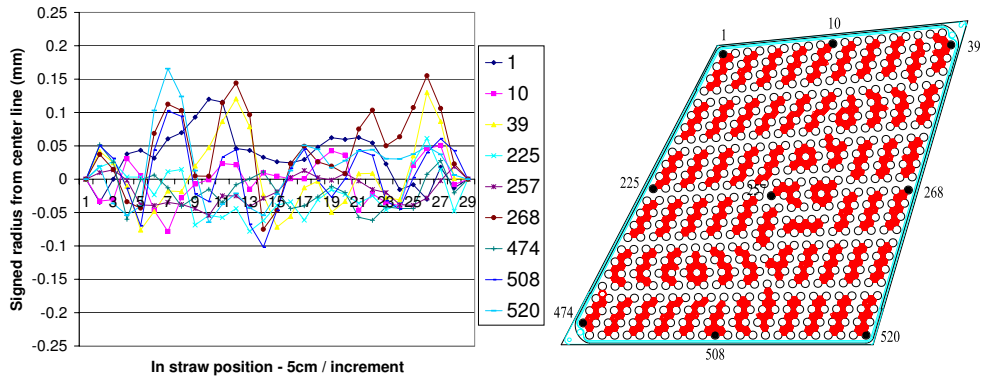

(b) Left: Deviation from center for the nine fiducial straws in a type 2 module. Right: Positions of the nine fiducial straws are shown in filled circles.

Figure 20. Laser survey system for straw straightness measurement.

4.3 Straw insertion

To avoid distorting radiator alignments and pushing radiator toward one end, straw insertion starts from the center of a module and goes outward in a spiral pattern. The direction of insertion is also alternated in sequential straws. When a straw is inserted, it goes through HV plates, radiators and alignment sheets several times. To avoid de-laminating the carbon fiber strips on a straw and to avoid any debris that may fall into it, a "straw insertion bullet" made of a Mylar sleeve over a rounded Delrin head is used to cap the straw end and guide it through the straw tunnel. Figure 21 shows a straw insertion bullet and the insertion path pattern.

With the straws inserted, the main body of a module is in place, however, at this stage, nothing has been glued and the process is reversible. Several tests are carried out, and any problem corrected, before proceeding:

1. The straw ends are inspected, making sure there is no damage and all 4 carbon fiber strips are present. Any stray radiator fibers that come to the HV plate are also removed. To do this, a stepping motor controlled camera is mounted at the straw end to step from straw to straw and the image is displayed on a TV screen for the operator to inspect.

2008 JINST 3 P02014

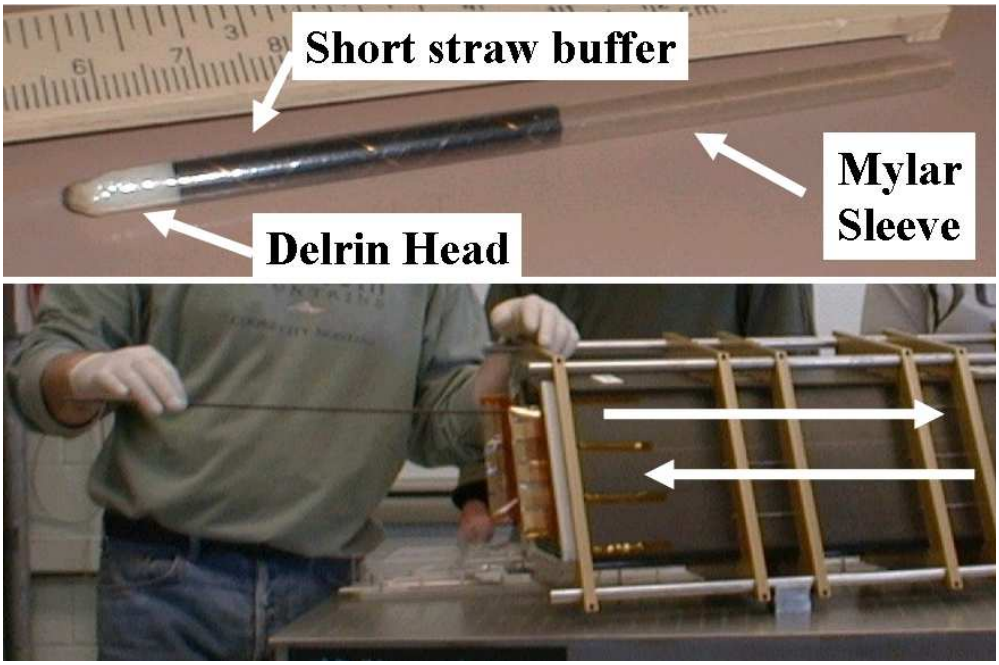

Figure 21. A straw insertion bullet, the straw insertion direction and sequence.

2. The nine stainless steel tubes are replaced by fiducial straws and surveyed again to ensure the alignment has not changed. After survey, the fiducial straws are replaced by normal straws.

3. A 2500 V test voltage is automatically cycled through all HV lines, one line at a time, by a PC controlled HV relay system to ensure no HV breakdown between straw groups, and, between straws and shell.

4.4 Assembly of HV endplates

With the HV plates referenced to the assembly frame, a few drops of super glue, 3M CA8, are used to fix the HV plates to the shell. Although it's possible to break the glue, this step effectively sets the length of the module and the position of the module mounting.

The straws need to be connected to the HV plate electrically and mechanically. This is done by using an Ultem "straw end-plug" and silver conductive glue. The straw end-plug is a cylinder with a cup shaped lip at one end, and housing the end wire support inside. A special tool is made to hold the end-plug under a glue dispenser and rotating it such that the glue surrounds the end-plug, and leaves an excess at one spot. When the end-plug is inserted into the straw, the excess is oriented toward the HV pad, it gets pushed out and flows around the cup shaped lip to the outside of the straw, and overflows to the HV pad on the HV plate. This way, the inside of the straw is electrically connected to the outside of the straw and connected to the HV pad that brings HV from the power supply. A stopper plate on the opposite end of the module is used to stop the straws from slipping while inserting the end-plugs from one end.

The silver glue takes 24 hours to cure. After one end is cured, resistance from the glued HV plate to the opposite open end of the individual straw is measured to check the glue quality. An 2500 V HV scan which steps through each individual HV line on HV while holding the rest of

2008 JINST 3 P02014

the lines on ground is repeated to ensure no stray silver glue is causing problem. The same gluing and testing process is repeated for the other side, except, when both ends of the straws are glued, resistance for individual straws are no longer available and the resistance for straws grouped in the same HV pad are measured.

After both ends of the straws are glued to the HV plate with conductive glue and tested. A layer of AY103 (Araldite 2019) epoxy is applied around the straw ends to provide mechanical strength. The low viscosity nature of AY103 also provides a first round of gas seal between straws and HV plate.

4.5 Gluing the shell

The shell is connected across the five alignment sheets and the two HV plates to form the structural support together with the carbon fiber re-enforced straws. For each alignment sheet, Araldite 2011 is applied along the four edges by inserting a flattened 1.5" long syringe tip between the shell and the alignment sheet through the shell holes cut out for the protruding alignment sheet tabs. This is a blind operation inside the shell and one has to be careful not to poke holes on the straws or apply the glue in the wrong place.

When the glue is cured the module structure is complete. The alignment sheet tabs are cut and the module is taken out from the assembly frame. A bead of Araldite 2011 is applied between the shell and the HV plate to strengthen the bond and as a seal for the purging gas volume confined in the shell.

To strengthen the gas seal of the ionization gas volume, the module is stood up vertically on a stand and a very low viscosity epoxy (Stycast® 1266) is injected through pre-cut holes on the shell to pot the back side of the HV plate with a 2.4 mm thick layer of glue. The glue slips through any crack or pin hole between the HV plate and the straws. This step completes the mechanical assembly of a module.

4.6 Finishing mechanical assembly

Before proceeding to stringing sense wires, a series of tests are carried out to check for the proper construction of the module. Glue blockage on mechanical pathways or electrical contacts are checked and corrected. Continuity of HV traces and HV stability are tested and repaired if needed. The gas tightness of the ionization gas volume is required to meet the specification of leaking less than 1 mbar/bar/min. For most modules the leak rate was measured below 0.1 mbar/bar/min.

After all the above test are passed, the pre-assembled tension plate is attached to the HV plate and the module is sent to the stringing station.

4.7 Wire stringing and testing

The presence of wire joints greatly complicates the stringing of sense wire into the modules, since the joint must be consistently located within 1 mm of the center wire support for straws with single wire joint, and, equally spaced for straws with double wire joints. Figure 4 shows positioning of wire joints inside the straws. The sense wire is pulled into the straws from "C" side to "A" side.

The first step in stringing a sense wire is to attach a "stopper" to the sense wire, which will be stopped at an external reference when the sense wire is pulled into the module. The external

2008 JINST 3 P02014

reference provides a stopping point at a known distance from the middle wire support and sets the wire joint position inside the straw. With a "pre-stringing" jig, the wire is put under tension and a stopper using eyelet and taper pin mechanism is attached at the trailing edge of the sense wire at a preset distance referenced to the leading edge of the wire joint. This distance is different for a single-joint or a double-joint wire and is set accordingly.

From the "A" side of the module (see figure 4), a leader wire consisting of 50 μm diameter copper/beryllium is blown through the straw using filtered and dried compressed air flowing through a tapered syringe tip inserted into the eyelet on the tension plate. The end of this leader wire exits the "C" side of the module and is attached to the sense wire by tying a knot. The leader and the sense wire together are then pulled back through the straw using a motorized spooling system until the stopper is stopped by the external reference. Then, a 70 g tension is applied to the sense wire from "A" side and the wire is pinned to tension plate on "C" side first and then on "A" side, and the tension is measured. The wire tension measurement was done by vibrating the module with a loudspeaker and sweeping an audio signal through the 100 – 200 Hz range. When the frequency matches the resonant frequency of the wire under tension, the wire vibration amplitude increases, causing a capacitance change in the wire/straw system which can be detected. This peak in the audio spectrum provides the wire tension, according to the relation:

$$T = 4\ell^2 f^2(\rho/980)$$

where T is the wire tension in grams, ℓ is the length of the vibrating wire segment 71 cm to the center wire supported, f is the resonant frequency in Hz, ρ is the linear density of the wire which in this case is 0.0001475 g/cm.

The stringing system is computer controlled and logs all stringing activity including restringing attempts and the wire tension measurements. If the tension is within the acceptable range of 55–80 g the wire excess is trimmed at the eyelets. If not, the "A" side taper pin can be removed and repinned to slightly change the tension, or the sense wire can be replaced. These procedures enabled $> 99\%$ of the straws to be strung, with the remainder having obstructions such as an irregularly shaped wire support or stray glue from mechanical construction.

After stringing is complete the wire tensions are measured again and logged. This is to verify that the cumulative effect of the tensions of all the wires has not caused dimensional changes in the module, and also to provide baseline data to be compared with that obtained during acceptance testing.

4.8 Finishing module assembly

After wire stringing, taper pins and eyelets on the tension plates as well as the edges between tension plate and HV plate are sealed with AY103. This completes the sealing of the ionization gas volume.

All holes on the shell, except the two reserved for purging gas fittings, are sealed with Kapton pads to complete the sealing of the purging gas volume.

A ground wire running from one tension plate to the other is soldered on to the tension plates and glued to the edges of the shell with conductive glue where carbon fiber is exposed. This completes the electrical ground path way of the module.

2008 JINST 3 P02014

5. Production testing

Before a module leaves the production site, a series of QA tests are performed. The data collected is the characteristic of a module and a part of a "passport" that travels with the module. Most of the tests are repeated when the module is received at CERN. The tests include:

- Re-measure wire tension
- Dimension tests
- Gas volume leak tests
- Signal and gain uniformity tests

5.1 Dimension test

The mounting holes of a module need to be in the right places so that the module can be mounted on the Barrel Support System. The dimension of a module also needs to fit inside a dimension envelope so that it doesn't interfere with others when mounted on the Barrel. To check this, the module is test mounted on a stand that simulates the Barrel Support System. This ensures the conformity of the mounting holes and the module length. The module is then checked against a flat surface and documented/corrected for any bulge that exceeds the envelope.

5.2 Gas volume leak test

The ionization gas volume is required to have a leak rate less than 1 mbar/bar/min. To test this, the ionization gas volume is pressurized with N_2 to 20 mbar and compared to a reference volume with a pressure gauge connected between the two volumes. The pressure difference between the module and the reference volume is recorded over time and calculated for the leak rate. The process often takes more than 12 hours. The environmental temperature, pressure, humidity are monitored for bias correction.

The ventilation gas volume is required to leak less than 200 mbar/bar/min. This is much less stringent than the ionization gas volume. Because the shell is easily deformed, this is measured by pressurizng ventilation gas volume with N_2 to 10 mbar and monitoring the pressure drop with a analogue gauge over 2–3 hours period of time.

5.3 Signal and gain measurement

To ensure a module can operate as it is designed to, the module is flushed with Ar(70%) - CO_2(30%) in the ionization gas volume and put on high voltage to sense signals generated by an X-ray source. Amplifiers and a DAQ readout system are set up to collect pulse charge information.

The first pass is a signal test to make sure that all channels are active and getting signals as expected. The second pass steps the X-ray source along the module to map out the gas gain variation along the sense wire. For gain mapping, the X-ray source is collimated and filtered with 50 μm Cu foil to concentrate on the 8 keV characteristic energy and reduce the energy spread.

The gas gain uniformity is important for stable operation of a module under LHC conditions, and for the TR function. However, non-uniformities also reflects construction irregularities in

2008 JINST 3 P02014

a module. Figure 22(a) shows a non-conforming straw. The spike in the middle indicates that the sense wire is not seated at the center of the middle wire support. This problem can often be corrected by re-stringing the wire. Figure 22(b) shows another non-conforming straw. The periodic humps indicate that the straw is bent between alignment planes. For this kind of straws, the wires are removed and the channels are not used.

6. Acceptance tests at CERN

This section presents a complete list of acceptance tests and quality control criteria used for the TRT Barrel modules. Many of these tests were first performed during module assembly but all were repeated during the quality control process at CERN for uniformity and conformity before the modules were accepted for insertion in the Barrel Support System.The first modules were qualified in 2003. All modules were qualifed in 2004 and were installed into the BSS in 2005. The completed Barrel TRT was installed in the ATLAS detector in August, 2006.

6.1 Quality control testing sequence

Each module upon arrival at CERN underwent the following quality control testing sequence. The tests themselves are described in details in the following sections.

1. Dimension checks
2. Tension test
3. Initial leak test
4. Initial HV checks
5. Rework: all miscellaneous repairs and restringing of identified problematic wires
6. Final HV checks
7. HV conditioning
8. Gain mapping
9. Final leak test for active gas and purging volumes
10. Weight
11. Quality control review

The results of the tension test and initial HV checks done at CERN as well as results from the gain mapping performed at the production sites were used to identify wires that needed to be replaced at CERN. A first leak check was also performed on the straw volume and the shell to identify leaky straws and leaky shells at the earliest possible stage. Replacement of known problematic wires and repairs for blocked cooling sleeves, blocked electronic sockets and leaky straws were performed before the module underwent the final HV checks. After rework, the module was tension and HV tested again before undergoing HV conditioning and gain mapping with the

2008 JINST 3 P02014

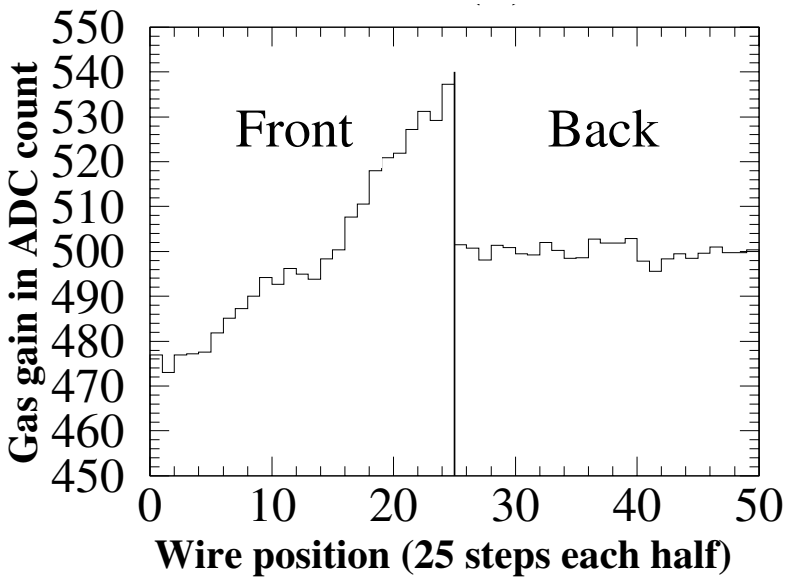

(a) A hung wire.

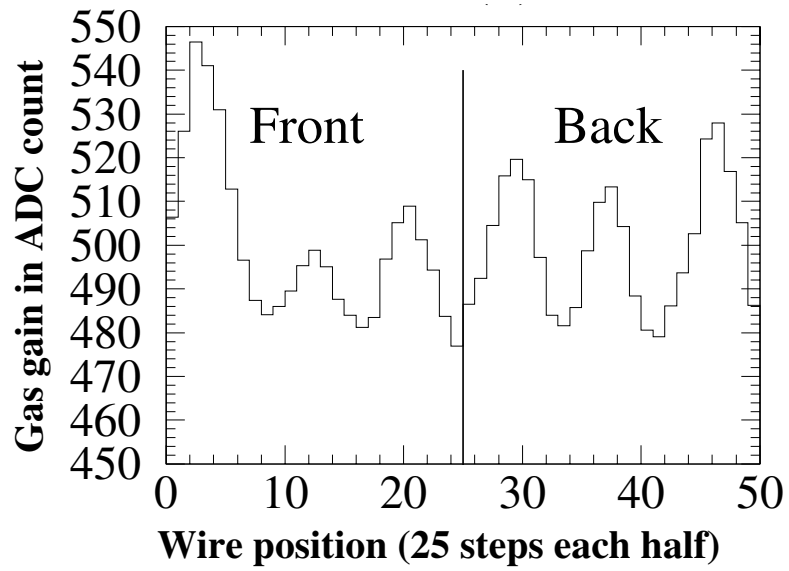

(b) A bent straw.

Figure 22. Gas gain variation along the sense wire. The step positions are fine tuned to equally distribute between dividers. (a) The peak at the center left is an indication that the sense wire was caught off-center at the middle wire support. However, the flat spectrum on the right indicates that on the other side of the middle wire support the wire exited the wire support normally from the center. (b) The peaks between dividers are indication that the straw is bent between divider planes.

Module Gain Mapper (MGM). When all tests and repairs were completed, the module was leak tested and certified for readiness before shipping it to the assembly building for installation on the Barrel Support System. All tests results were compiled in a "module passport", where a summary of all results, anomalies, repairs and dead channels was recorded.

2008 JINST 3 P02014

6.2 Dimension checks

All main dimension parameters were re-measured once the Barrel modules arrived at CERN. The length of each of the three sides measured had to be between 1462.0 mm and 1464.0 mm. All modules were found to be between 1461.5 and 1462.95 mm. A small shim was added for the shorter modules during insertion on the Barrel Support System. Bulges in the shell could not exceed 0.8 mm and twists of one tension plate with respect to the other had to be less than 1.0 mm; twists larger than 0.2 mm were recorded in the module passport. All bulges and twists found were within these limits. The two cooling sleeves were checked for blockages and repaired if needed before undergoing the HV tests.

6.3 Wire tension measurements

The tension was re-measured at CERN for each wire to ensure that no wire had slipped during shipment. This value was compared to the tension measurement taken at the production site after stringing. The tension was required to be larger than 47 g and less than 100 g, and with no more than 5 g change since stringing, or show a tension difference between the front and back wire segments greater than 8 g. Out of the 58592 wires tested, 142 wires (0.24%) were found to be outside these specifications and were replaced, as well as 10 wires (0.02%) that had broken or slipped out of the wire-joint during shipment. Only two wires had to be permanently removed due to tension anomalies. In some rare cases, the spectrum showed a double peak, indicating an electrical connection with one or many nearby wires due to a piece of wire caught between the tension plate and the HV plate. The extraneous piece of wire had to be removed and these channels could be restrung.

6.4 High voltage tests

6.4.1 Check of all electrical connections

The electrical connections between each capacitor barrel pin and the HV trace on the Kapton connector were all checked for continuity to ensure there was no damage to the HV distribution chain. Broken traces were noted in the module passport. Eight modules were found with a broken HV trace and were mounted on the Barrel Support System such that the fusebox was connected to the undammaged Kapton connector at the other end. We also checked the connection for the ground wire between the front and back tension plates and recorded in the module passport all HV groups that were inadvertently interconnected according to the production site passport. These groups were detected while testing the HV plates by applying 2000 V on one HV pad and holding all others to ground.

6.4.2 HV checks

Both the initial and final HV checks were conducted with Ar/CO_2 in the active gas volume while flushing with CO_2 in the radiator volume. All wires were kept at ground potential while -1550 V was applied to the straws. This corresponded to a gain of 10.0×10^4, namely four times the nominal gain. The module was prepared for HV checks by flushing dry CO_2 for several days in the radiator volume prior to testing to reduce the water content. The relative humidity level in the laboratory

2008 JINST 3 P02014

itself was maintained at or below 30%. For both tests, we required that each wire held -1550 V without tripping the HV power supply at a limit of 20 μA $\times$ 5 sec for a minimum of three days.

6.4.3 Initial HV checks

Non-complying wires identified during the initial HV checks were replaced. The leakage current was required to be below 20 nA per module at -1550 V (without any capacitors). Typically, leakage currents of the order of 10 nA per module were measured. This varied slightly between modules but largely depended upon the relative humidity level in the lab. To cure wires drawing excess current or modules having too many trips during the HV checks, reverse-voltage was applied at a maximum of +1300 V. The duration depended on the current behavior and was usually of the order of 30-60 minutes. This helped removed residual dirt or contaminants on the wires, reducing the overall number of trips and amount of leakage current. In total, 300 wires that could not be cured by reverse-voltage or caused repeated discharges even after reverse voltage treatment were replaced following the initial HV checks and were found to satisfy the minimum criteria in subsequent HV tests.

6.4.4 Final HV checks

The module was given a final HV check under the same conditions as the intial HV checks after all rework was completed. An additional 222 wires that caused trips during this test were removed permanently, including 150 replaced wires that kept giving HV problems.

6.4.5 Rework

Table 3 summarizes the causes for wire replacement that took place prior to the final HV checks. A third of the wires needing replacement were detected during the initial gain mapping in the U.S. prior to shipment to CERN. The vast majority of them were wires that got hung on the central or end twister, causing a large wire offset. Only a handful of hung wires could not be restrung successfully due to a problem in the twister itself.

Another third of the replaced wires were problematic wires identified during the initial HV tests. These wires either had a defect, a kink or were simply dirty. Replacing the wire cured the problem. On the other hand, some replaced wires kept causing discharges, most likely due to a problem in the straw itself or in one of the twisters. These wires were found during the final HV checks and had to be permanetly removed.

Many channels proved difficult to string at the production site, often due to pieces of wires or small debris caught inside the straw. In many of these cases, small pieces of wires could be retrieved by "fishing" inside the straw with a piece of twisted $\sim 50-100\,\mu m$ wire. By twirling it inside the straw, the small pieces of wire would get caught on it and could be pulled out. This operation was successful on 194 of the 347 channels left unstrung at the production site. In some cases, tiny pieces of wire, solder or even long sections of wire had fallen between the tension plate and HV plate, causing HV shorts and/or occasionnal discharges. Some were identified during HV checks or during the tension test. Some were located using an endoscope through an eyelet and fished out using a tiny hook on a piece of lead wire, while others were retrieved using a vacuum pump or even using a large industrial vacuum cleaner on one of the active gas inlets. Some wires were temporarily removed to allow various repairs. A summary of the causes for wire replacement is given in table 3.

2008 JINST 3 P02014

Table 3. Total number of wires successfully replaced for the 111 modules tested.

Cause for wire replacement	# wires	% of total wires
Problem found during gain mapping in the USA	352	0.60%
HV problem found during early HV checks	300	0.51%
Straw left unstrung at production site	194	0.33%
Tension too low or too high, slippage, front/back difference	142	0.24%
Removed temporarily to fish out pieces of wires	80	0.14%
Broken wires	10	0.02%
Removed temporarily to fix a straw leak	2	$< 0.01\%$
Total: 111 modules with 58592 straws	1055	1.80%

6.5 HV conditioning

The HV conditioning took place over a four week period after the final HV checks and all problematic wires had been removed. The purpose of the conditioning step was to ensure that no problematic channel had been missed during the HV checks. The HV and gas conditions used for this test were the same as the previous HV checks. The number of discharges and the leakage current was monitored for the whole module over the entire period. Individual channels were not monitored during this test. A module was required to hold -1550 V without discharges for the last two weeks. Occasional discharges during the first two weeks were attributred to some initial cleaning processes. The leakage current was required to be below 20 nA per module at -1550 V (without any capacitors). If a module failed to satisfy these criteria, it was returned to the HV test station for investigation. Problematic wires were removed and the module was conditioned a second time.

6.5.1 Leakage current at -2000 V with CO_2 in the straws

After one month of HV conditioning performed as described above, pure CO_2 was circulated in the straws overnight. We then measured the leakage current after 15 minutes while applying -2000 V on the straws with all wires and the shell grounded. The purpose was to detect any HV problems in the absence of amplification in the active volume. The leakage current had to be below 20 nA per module. Six wires shorted out in CO_2 while applying between -1900 and -2000 V on the straws and were removed.

6.5.2 Gain mapping

Modules were placed in the Module Gain Mapper (MGM) and supplied with Ar(70%)/CO_2(30%) mixture in the ionization gas volume and CO_2 in the purging gas volume. The MGM scanned a 12 keV X-Ray beam (from a bromine transition) along the full length of each module. All module channels were instrumented and a switching network steered signals from sixteen channels at a time to histogramming ADCs. Fifty points on each straw were sampled for gain. This gain mapping took place either before or after HV conditioning, to ensure a steady module flow on every test station. The wire acceptance criteria were similar to those used after gain mapping in the U.S.: gain variation less than 8 % and peak width less than 7.5 %. In addition, wires having a gain variation higher than 7 % were also examined to ensure that S/A was less than 25 %, where S

2008 JINST 3 P02014

Table 4. Dead channel statistics.

Cause for removal	# wires	% of dead channels	% of entire TRT Barrel
Bent straw	349	44.9 %	0.66 %
HV problems	222	28.6 %	0.42 %
Unstrung at production site	153	19.7 %	0.29 %
Wire offset	37	4.8 %	0.07 %
Broken socket	14	1.8 %	0.03 %
Tension	2	0.3 %	< 0.01 %
Total out of 525442 wires	777	100 %	1.48 %

represents the half-width at 20 % of maximum height of the spectrum of the highest gain point and A the maximum amplitude. The S/A value was corrected for ADC offsets. New wires and wires that did not receive a valid measurement during gain mapping in the U.S. were particularly scrutinized. Non-conforming wires were removed.

At this stage, the module had reached its final state and all identified problem channels had had their wires removed. The largest number of dead channels comes from bent straws (44.9 %), mostly in Type 3 modules where 74 % of all bent straws were found. These straws have large wire offsets and large gain variations, compromising HV stability during operation and hence, had to be removed. The second largest category comes from channels having HV problems, either identified at CERN during acceptance tests (28.6 %) or at the production site (19.7 %). Table 4 summarizes the final number of dead channels in the TRT Barrel and the various causes for wire removal. In total, 98.53 % of all TRT Barrel channels were fully operational at the time of installation.

6.6 Final fluid-tightness tests

6.6.1 Active gas volume

For the active gas, the target was to achieve a leak rate below 0.1 mbar/min/bar. Nevertheless, modules with leak rates up to a factor 10 times larger were accepted. The test was done with Argon at 20 mbar (0.3 psig) over-pressure and conducted over a 12 to 16-hour period. This test was done after all non-conforming wires found during the HV conditioning and found with the Module Gain Mapper had been removed and sealed. All but 15 modules had a leak rate below 0.1 mbar/bar/min. The remaining 15 modules had leak rates up to 0.6 mbar/bar/min. After capacitor insertion, the leak rate was remeasured and 30 modules exceeded the target value of 0.1 mbar/bar/min, but only five of these modules had leak rates between 0.3 and 0.6 mbar/bar/min.

6.6.2 Ventilation gas volume

The cooling/ventilation gas connections and seals had to achieve gas leak rates below 1 mbar/min at about 5 mbar over-pressure. The test was done by pressurizing the module with about 10 mbar of water column. The decay time had to be greater than 5 minutes. Non-conforming modules were repaired and all satisfied this criterion.

2008 JINST 3 P02014

6.7 Module acceptance passports and Quality Circle review

The module passport contains the results of all acceptance tests, anomalies and repairs done at CERN as well as selected information from the production sites on which rework and repair decisions were based. The module passport contains:

- A summary of all dead channels,
- A summary of all remaining anomalies either reported by the production sites and not fixed at CERN, or discovered at CERN and found impossible to repair,
- A report on dimensions checks and final module weight,
- A comparative study of tension data between the production site and CERN,
- A summary of gain mapping results in the United States and at CERN showing a 2-D map of the gain variations for all wire segments (front and back) and a summary table of the status of all wires having a gain variation of more than 8%,
- A summary of all repairs, including a list of replaced wires and removed wires,
- A complete report on HV tests, HV conditioning, leakage currents without capacitors and anomalies noted during the various HV tests,
- The leak rate for the active gas volume before and after capacitor insertion.

The passports are kept at http://trt-wts.web.cern.ch/trt-wts/passp/blogin.html. The information resides in a CERN-based Oracle database. A web interface allowed users to enter or review information from anywhere. Based on the module passport, a Quality Circle composed of several physicists reviewed the information for each module and decided if it could be used in the TRT Barrel. Of the 111 modules shipped to CERN, the 96 best modules were installed on the Barrel Support System whereas an additionnal seven modules satisfying all acceptance criteria were prepared as spares. The remaining four modules were rejected and will be used for testing and educational purpose.

7. Beam test performance

TRT Barrel performance was evaluated using electron, pion and muon beams with energies from 1 - 300 GeV. For this purpose two TRT barrel "phi" stacks, corresponding to 1/16 of the final Barrel, were assembled and installed on the H8 line of CERN SPS, figure 23. The detector was equipped with the final TRT readout electronics. This test was completed in August, 2006.

In order to obtain a precise particle trajectory and identify the beam particle auxiliary detectors were used. A three plane silicon telescope with intrinsic resolution of $10\,\mu m$ was used as an external tracking to define the beam trajectory. A Cherenkov counter system and preshower and lead glass calorimeter were used to identify the particles. Measurements with TRT modules were carried out using the baseline mixture 70%Xe+27%CO_2 +3%O_2.

One of the most important parameters which defines the detector performance is the drift-time accuracy. This is defined as the sigma of the distribution of the track residuals by comparing the

2008 JINST 3 P02014

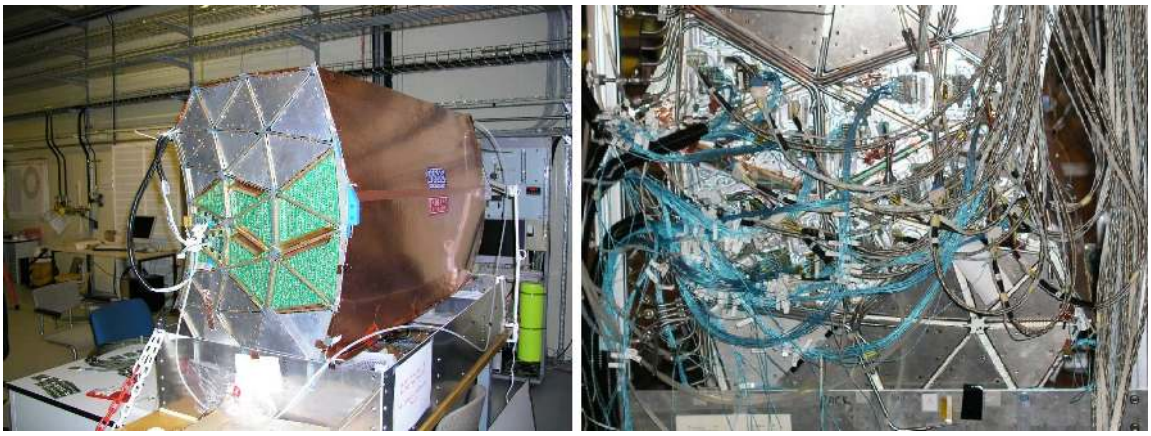

Figure 23. Two "phi" stacks of the TRT Barrel installed in H8 beam line. Left picture - preparation for the tests beam. Right picture - TRT Barrel installed on the beam line and equipped with front-end electronics.

space points measured using drift-time information to the actual particle position projected by the silicon-telescope. Another critical parameter is the TRT drift-time efficiency which is defined as the probability for finding the drift-time measurement hit within a $\pm 2.5\sigma$ window from the beam particle track. The uniformity of these parameters across the detector reflects its production quality. On the top plot of figure 24 the total straw efficiency and the drift-time measurement efficiency are shown as a function of Barrel straw layer number (counting from inner to outer radius). The bottom plot shows drift-time accuracy as a function of the same parameter. All these values are well within the specifications presented in the TDR.

The drift-time accuracy for the first 9 layers is $130\,\mu$m while it is $137\,\mu$m for following layers. This is explained by the fact that the active wire for the first 9 layers is shorter than that for the other layers, resulting in a shorter time difference between the direct signal and the reflected signal from the wire joint termination. Wire position accuracy is a critical parameter for the track reconstruction procedure. Figure 25 shows wire placement deviation from its nominal geometrical position as a function of the TRT Barrel depth measured with a beam of 80 GeV pions. It can be seen that the TRT module production accuracy is very good and this deviation is less than $50\,\mu$m.

Particle identification properties of the TRT Barrel using transition radiation were studied at several different beam energies. Here we report studies on 20 GeV beam energy. Extensive MC and test beam studies at this energy had been carried out in the past and published in the TDR. The results are shown in figure 26. On this figure the pion rejection power is shown as a function of the high level threshold at two beam positions along the straw. The upper points are when beam particles crossed the Barrel module 40 cm from its edge. At this position the first 9 straw layers are not active. The lower points are when the beam was positioned 20 cm from the edge of the Barrel where all 73 straw layers are active.

As seen in this figure the best particle identification properties for the TRT Barrel are at a threshold of about 7 keV. Pion efficiency in that case is $1.5-3\%$ at 90% of the electron efficiency.

2008 JINST 3 P02014

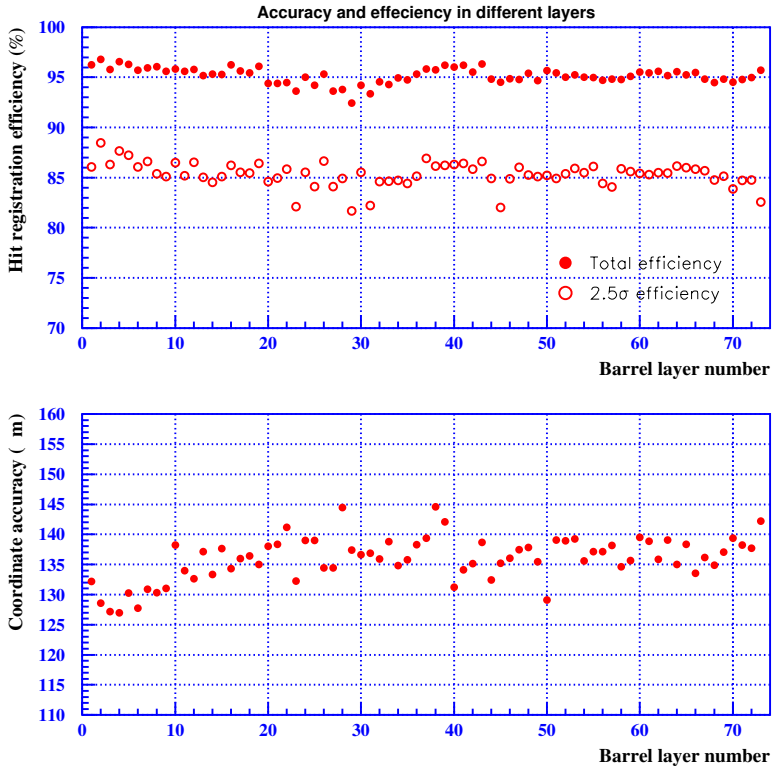

Figure 24. Hit efficiency registration (top plot) and drift time accuracy (bottom plot) as a function of the Barrel straw number for incident pions of 80 GeV.

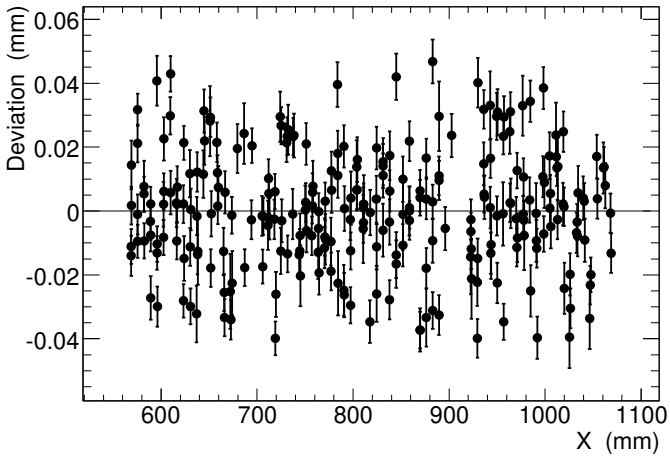

Figure 25. Wire placement deviation as a function of the TRT Barrel depth.

8. Summary

We have completed the construction of the TRT Barrel for the ATLAS Inner Detector. A total of 111 modules were constructed over the period 1998 to 2003 at three sites within the United

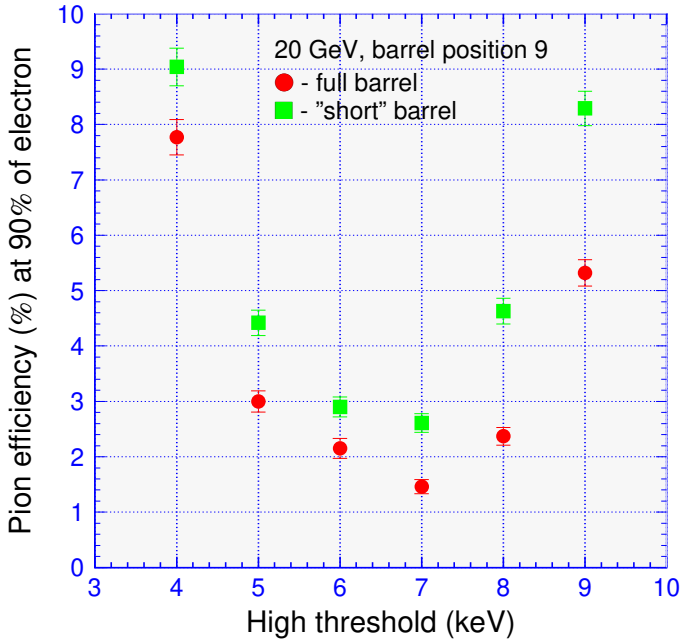

Figure 26. Electron/pion rejection power as a function of the high level threshold. Red markers: all Barrel straw layers are active. Green markers: particle crosses the Barrel in the central area where the first 9 layers do not have active anode wires.

States. These modules were extensively tested and the 32 best of each of the three types were selected for assembly in the Barrel Tracker. The 96 modules in the BSS frame have been tested as a unit, and the associated services such as HV, active gas, and cooling have been contructed to operate and take data. At the time of assembly 98.5 % of the 52,544 drift tubes were operational. Individual modules have been tested in the CERN test beam. The module performance was within specification for tracking resolution and transition radiation performance.

Acknowledgments

The research described in this publication was partly supported by following funding agencies: the European Union (DGXII), the International Science Foundation, the Danish Natural Science Research Council, the Swedish Research Council, the Knut and Alice Wallenberg Foundation, the Ministry of Science and Higher Education, Poland, the International Science and Technology Centre, the Civil Research and Development Foundation and grants from the U.S. Department of Energy and the U.S. National Science Foundation, the Natural Science and Engineering Research Council of Canada, the Ministry of Education and Science of the Russian Federation, the Academy of Science of the Russian Federation, the International Association for the Promotion of Cooperation with Scientists from the new Independent States of the former Soviet Union, The Turkish Atomic Energy Authority.

2008 JINST 3 P02014

References

[1] ATLAS collaboration, *Atlas Inner Detector Technical Design Report. Vol. 1*, ATLAS TDR 4, CERN-LHCC-97-16, CERN (1997).

[2] ATLAS collaboration, *Atlas Inner Detector Technical Design Report. Vol. 2*, ATLAS TDR 5, CERN-LHCC-97-17, CERN (1997).

[3] V. Polychronakos et al., *Integrated high-rate transition radiation detector and tracking chamber for the LHC*, Detector R & D proposal, CERN-DRDC-90-38, CERN (1990).

[4] V. Polychronakos et al., *Integrated transition radiation detector and tracking detector for LHC*, RD6 Status Report, CERN-DRDC-91-47, CERN (1991).

[5] V. Commishau et. al., *Integrated transition radiation detector and tracking detector for LHC (transition radiation tracker)*, RD6 Status Report, CERN-DRDC-93-46, CERN (1993).

[6] T. Akesson et al., *Study of straw proportional tubes for a transition radiation detector / tracker at LHC*, CERN-PPE/94-224, *Nucl. Instrum. Meth.* **A 361** (1995) 440.

[7] T. Akesson et al., *Particle identification performance of a straw transition radiation tracker prototype*, *Nucl. Instrum. Meth.* **A 372** (1996) 70.

[8] M. Stavrianakou, *Prototype results from a straw tracker with integrated transition radiation capability for the atlas experiment at the LHC*, *Nucl. Instrum. Meth.* **A 360** (1995) 57.

[9] RD6 collaboration, W. Fuchs et al., *A straw transition radiation tracker for the LHC*, *Nucl. Phys. Proc. Suppl.* **44** (1995) 258.

[10] ATLAS TRT collaboration, T. Akesson et al., *Electron identification with a prototype of the transition radiation tracker for the ATLAS experiment*, *Nucl. Instrum. Meth.* **A 412** (1998) 200.

[11] T. Akesson et al., RD6 Collaboration, *The ATLAS TRT straw proportional tubes: Performance at very high counting rate*, *Nucl. Instrum. Meth.* **A 367** (1995) 143.

[12] ATLAS TRT collaboration, T. Akesson et al., *Straw tube drift-time properties and electronics parameters for the ATLAS TRT detector*, *Nucl. Instrum. Meth.* **A 449** (2000) 446.

[13] M. Capeans et al., *Recent aging studies for the ATLAS transition radiation tracker*, *IEEE Trans. Nucl. Sci.* **51** (2004) 960.

[14] ATLAS TRT collaboration, T. Akesson et al., *Operation of the atlas transition radiation tracker under very high irradiation at the cern LHC*, *Nucl. Instrum. Meth.* **A 522** (2004) 25.

[15] ATLAS TRT collaboration, G.F. Tartarelli et al., *The ATLAS Transition Radiation Tracker*, *Nucl. Phys. Proc. Suppl.* **78** (1999) 348.

[16] ATLAS TRT collaboration, A. Romaniouk et al., *The ATLAS Transition Radiation straw Tracker (or TRT): present status and performance*, *Nucl. Phys. Proc. Suppl.* **61B** (1998) 277.

[17] A.O.Golunov et al., *An automatic system for controlling the quality of straws installed in the ATLAS TRT detector*, *Nucl. Instrum. Meth.* **A 524** (2004) 142.

[18] ATLAS TRT collaboration, M. Capeans, *The transition radiation tracker of the ATLAS experiment*, *IEEE Trans. Nucl. Sci.* **51** (2004) 994.

[19] ATLAS TRT collaboration, T. Akesson et al., *Status of design and construction of the Transition Radiation Tracker (TRT) for the ATLAS experiment at the LHC*, *Nucl. Instrum. Meth.* **A 522** (2004) 131.

2008 JINST 3 P02014

[20] P. Cwetanski et al., *Acceptance tests and criteria of the ATLAS transition radiation tracker*, *IEEE Trans. Nucl. Sci.* **52** (2005) 2911.

[21] ATLAS collaboration, *Atlas inner detector technical design report Vol. 2*, ATLAS TDR 5, CERN-LHCC-97-17, CERN (1997).

[22] ATLAS TRT collaboration, *The ATLAS Transition Radiation Tracker (TRT) proportional drift tube: design and performance*, to be published in JINST.

[23] ORPE Technologiya, Obninsk, Russia, http://www.technologiya.ru/.

[24] Composite Horizons, Inc, Signal Hill, California, http://www.chi-covina.com/.

[25] Chapman-Lake Instrument Corporation, Bloomington, IN, http://www.chapmanlakeinstrument.com/.

[26] Freudenberg Vliesstoffe KG, D-69469 Weinheim, Germany, http://www.freudenberg.com/.

[27] The Breiner Company, Avon, IN, http://www.breinerco.com/.

[28] Optical Gaging Products Inc., model: Avant-600, http://www.ogpnet.com/.

[29] American Circuits Inc., 513 West 24th St., Charlotte, NC, http://www.americancircuits.com/.

[30] Saklax Manufacturing Company, 1346 Blue Hills Ave. #B, Bloomfield, CT 06002, U.S.A.

[31] ATLAS TRT collaboration, *The ATLAS TRT electronics*, submitted to JINST.

[32] N. Dressnandt, N. Lam, F.M. Newcomer, R. Van Berg and H.H. Williams, *Implementation of the ASDBLR straw tube readout ASIC in DMILL technology*, *IEEE Trans. Nucl. Sci.* **48** (2001) 1239.

[33] TRI GON Precision, Inc., 820 South Sahwatch, Colorado Springs, CO 80903, U.S.A., http://www.tri-gon.com/.

[34] Rubis Precis, F-25140 Charquemont, France, http://www.rubis-precis.com/.

[35] Swiss Screw Products Inc., 339 Mathew St., Santa Clara, CA 95050, U.S.A., http://www.swissscrew.com/.

[36] S.H.Oh, A.T.Goshaw, and W.J.Robertson, *Construction and performance of a 2.7 m long straw drift tube prototype chamber for the SSC*, *Nucl. Instrum. Meth.* **A 309** (1991) 368.

[37] Petersburg Nuclear Physics Institute (PNPI), Russian Academy of Science, Gatchina, St. Petersburg, Russia, http://www.pnpi.spb.ru/.

[38] Joint Institute for Nuclear Research (JINR), Dubna, Moscow Region, Russia, http://www.jinr.ru/.

[39] Richland Glass Co., 1640 South West Blvd., Vineland, NJ 08360, U.S.A., http://www.richlandglass.com/.

[40] Micro-electronics Department, Moscow Engineering Physics Institute (MEPHI), Russia, http://www.mephi.ru/eng/second.html.

[41] J. Fowler et al., Duke Atlas Group, *Fuse box design report*, ATLAS TRT internal note: Dukhep-2004-12-13.

[42] A.Catinaccio, A.Angantyr and H.Danielsson, *FEA of the Atlas ID Barrel Support Structure*, CERN EDMS ATL-IC-EA-0001.

[43] J.Fowler, A.Catinaccio, *Quality Control of TRT Barrel Support Structure Inner Cylinder*, CERN EDMS ATL-IC-QC-0001.

2008 JINST 3 P02014